CHAPTER-5

LITHOFACIES AND INORGANIC GEOCHEMISTRY

5.1 INTRODUCTION

The term "facies" originated from the Latin word "facia," which refers to the outward appearance or visual aspect of anything, introduced by Nicholas Steno in 1669. Walther (1894) later defined facies as the collective combination of all fundamental attributes of a sedimentary rock. Moore (1949) gave a precise definition of lithofacies, “The rock record of any sedimentary environment, including both physical and organic characters, is designated by the term “lithofacies’. The term 'lithofacies' refers to the complete set of lithological features of sedimentary rock. The analysis of lithofacies involves a systematic examination of sedimentary rock characteristics such as grain size, mineral composition, sedimentary structures, and fossils, facilitating their categorization into discrete lithofacies types (Miall, 1985). This methodology serves as a fundamental tool in sedimentary geology, enabling precise interpretations of ancient environments and depositional settings based on the spatial and temporal variations of lithofacies within sedimentary sequences (Miall, 1985). Through lithofacies analysis, geologists gain invaluable insights into the complex interplay of geological processes, aiding in the reconstruction of Earth's geological history and the understanding of past environmental conditions (Nichols, 2009). Within the scope of this study, the terms 'facies' or 'lithofacies' are employed in a sedimentological context, emphasizing field-based and petrographic-based parameters for their identification and characterization (de Raaf et al., 1965; Walker, 1992). Lithofacies analysis hinges upon field-based criteria such as geometry, interbed relationships, lithological variations through depth, grain size, primary sedimentary structures, fossil content and petrographic examination. The investigation delved into detailed examinations of individual facies, leading to the determination of distinct depositional environments associated with each facies. Through field and petrographic analyses, sedimentary facies are systematically identified and interpretations are derived for their respective depositional settings for both Ninama and Chotila Basin.

The outcrops of the Ninama and Chotila Basin are thoroughly observed, measured, documented, sampled, and logged for detailed geological investigation. The sedimentary layers were mapped, and their field observations were recorded for macroscopic sedimentary textures and structures. A total of 162 samples were collected, more than 70 thin sections were made and thoroughly examined for mineralogical and textural parameters to determine the lithofacies. Leica MC 120 HD polarizing microscope with various magnifications of the objective lens (2.5×, 4×, 10× and 40×) and 10× eyepiece was used to study the petrography. The carbonate lithofacies and microfacies are named according to Dunham (1962), Embry and Klovan (1971) and Flügel (2010), sandstone lithofacies according to Dott (1964) and shale lithofacies according to Picard (1971) and Stow (1981) classification schemes.

5.2 FACIES DESCRIPTION

5.2.1 NINAMA BASIN

The facies analysis of the 39m thick Ninama Basin sequence of Sukhbhadar Formation and Ninama Limestone has resulted in seven lithofacies from the clastic and carbonate rocks (Fig. 5.1, Table 5.1).

Sr. No.	Lithofacies	Description
1.	Grey shale - GSH	Beige to grey in colour, well laminated and stratified, intercalated with SM and LGW. Variable in appearance, inconsequential amount of silt and sand-sized quartz.
2.	Calcareous shale - CSH	Yellow to buff coloured, finely laminated to thinly bedded layers, highly friable.
3.	Silty mudstone - SM	Reddish brown coloured, polygonal appearance due to shrinkage cracks, dominated by mud with some silt sized quartz.
4.	Lithic greywacke -LGW	Greyish to black coloured, coarse grained, dominated by volcanic rock fragments, quartz grains which are poorly sorted in nature.
5.	Grey black limestone - GBL	Grey to black coloured, massive, highly compact and jointed limestone with occasional chertification, organic matter and iron oxide. Mudstone microfacies.
6.	Cherty limestone - CL	Yellow to buff coloured, irregularly laminated and otherwise, cherty limestone, thinly bedded in nature. Microfacies- Pelloidal wackestone-packstone microfacies, Bioclastic bindstone microfacies, Cone in cone calcitic microfacies.
7.	Marlite - ML	Blocky and massive limestone, yellow to light orange in colour, thickly bedded, containing moderate amounts of argillaceous matrix. Cladoceran bindstone microfacies.

Table 5.1 Clastic and carbonate lithofacies of the Ninama Basin.

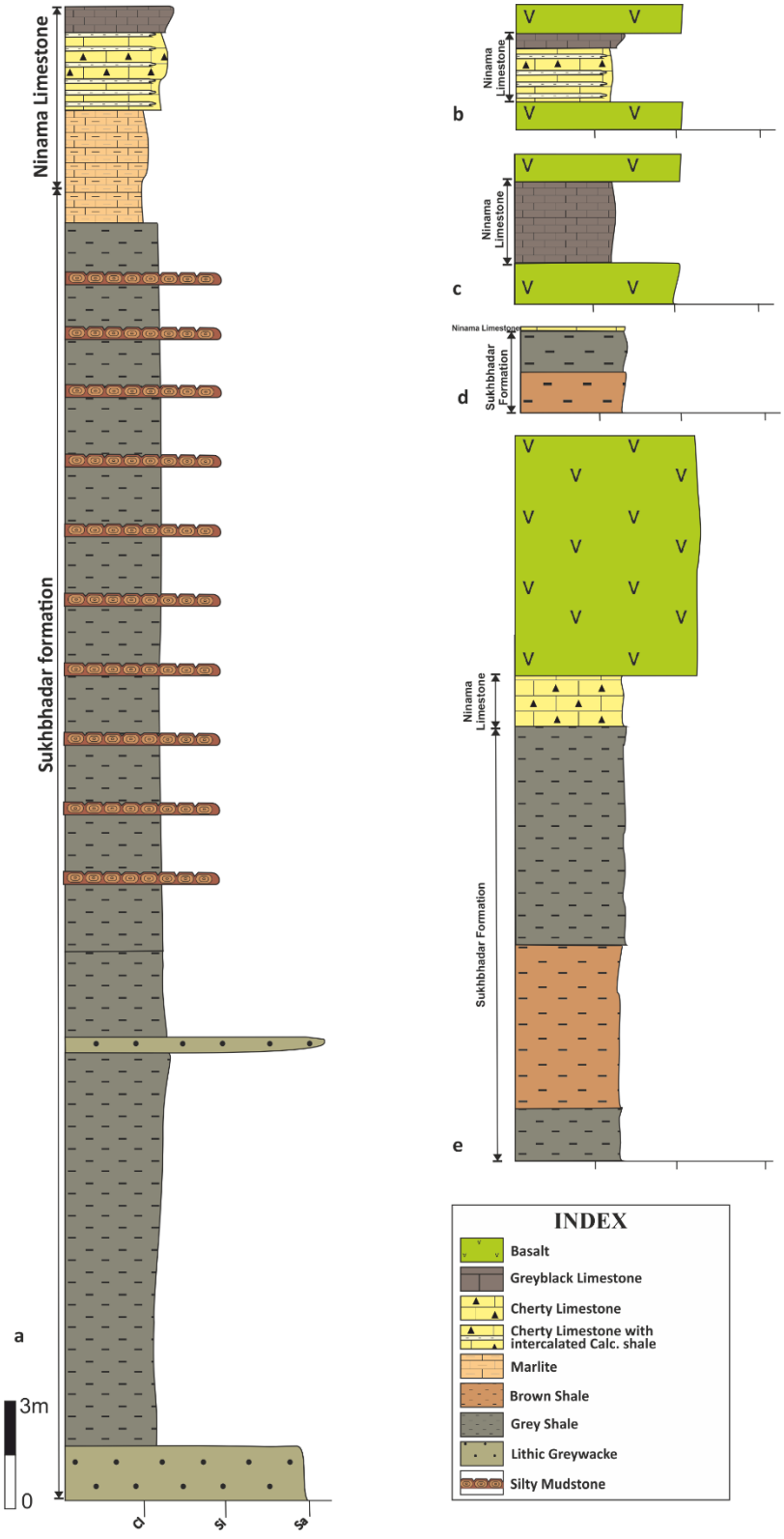

Fig. 5.1 Measured lithologs of the Ninama Basin intertrappean sequence show the lithofacies distribution. a. Composite litholog of the Ninama section, Ninama village. b. Shekhdod hill section, Shekhdod village. c. Moti Lakhavad section, Moti Lakhavad village. d. Motamatra hill section, Motamatra village and e. Motamatra well section, Motamatra village.

5.2.1.1 Clastic Lithofacies

5.2.1.1.1 Grey Shale Facies (GSH)

Description: This facies is well exposed on the right bank of the Sukhbhadar river near Ninama village (Plate 5.1a) and is also observed in the well section near Motamatra village. It is 18m thick, consisting of laminated, stratified and fissile shales mainly observed in the Sukhbhadar Formation. It shows colour variations, laterally and vertically, and appears in shades of beige, brown and grey (Plate 5.1b). It is dominated by fine clay size clastic grains with the subordinate amount of the silt size fraction which developed the fissility. The proportion of clay and silt-sized grains are unevenly distributed laterally and vertically and have controlled the laminations and fissility. Laterally, towards the SE, near Motamatra the facies become hard, compact, and laminated in nature.

Interpretation: The thick sequence of the fine-grain clastic sediments suggests deposition took place in calm to low energy conditions. The lateral occurrence of the discontinuous rhythmic laminations of silt and clay suggests an intermittent supply of the sediments. The development of the thick sequence is due to a prolonged dormant period of the lava flow where the deep paleolake has received the sediments continuously in the topographic low of the Deccan Traps. The clay size particles were deposited in calm conditions while silt size was deposited in the low-energy offshore environment of the paleolake (Einsele 1992).

5.2.1.1.2 Calcareous Shale Facies (CSH)

Description: The calcareous shale lithofacies occur rhythmically with Marlite (ML) and Cherty Limestone (CL) lithofacies (Plate 5.1c, d). The facies consist of a few laminated to thinly bedded layers, which are highly friable and yellow to buff in colour. The proportion of clastic and carbonate usually shows consistency but is dominated by fine clastics. They are highly variable in nature, with discontinuous lateral and vertical extensions (Plate 5.1c, d). This facies occurs towards the upper part Ninama Limestone sequence and is observed around Ninama village and Shekhdod village.

Interpretation: The CSH is characterized by mixed fine-grained clastic and carbonate sediments suggesting intermittent high fine-grained clastic influx which partially halted carbonate deposition. The variable thickness of the beds and their horizontal discontinuity reflect dynamicity in near-shore settings of the paleolake.

Plate 5.1 a. The exposure of grey shale facies (GSH) on the right bank of the Sukhbhadar River near Ninama village. b. Laminated SH and Marlite (ML) facies exposed above the shale facies. c and d. Exposures of the calcareous shale (CSH) and cherty limestone (CL) facies. e. Thinly bedded silty mudstone (SM) facies shows gradational contact with shale facies. Photomicrographs of SM. f. Silt-sized quartz grains in a muddy matrix with iron oxide. g. Subordinate amount of quartz grains in the mud with iron oxide. h. Bands of lithic greywacke (LGW) facies are exposed in the dug well near Ninama village. Photomicrograph of lithic greywacke showing, i. Volcanic fragment (basalt), quartz grains with cleavable calcite and j. Texturally immature shows the cleavable calcite, iron oxide, broken quartz grains, and volcanic fragments, (Cc- Cleavable calcite, Qz- Quartz, Vf- Volcanic fragment, Io- Iron oxide, M- Mud; Scale- person height- 175cm, ruler length- 30cm).

5.2.1.1.3 Silty Mudstone Facies (SM)

Description: This facies is reddish brown in colour and occurs as a few cm thick bands at intervals of 100-120cm, at multiple levels in the Sukhbhadar Formation (Fig. 5.2a). The SM facies consists of high amounts of mud as compared to silt. It is characterized by shrinkage cracks, resulting in three-dimensional polygonal structures which are variable in size (Plate 5.1e). Petrographically SM is composed of a fine muddy matrix with silt-sized quartz grains (Plate 5.1f, g). The proportion of silt varies widely, usually less than 50% and shows a wide range of grain size from very coarse to fine. The quartz grains are subangular to sub-rounded in nature, with low sphericity and floating in the matrix (Plate 5.1f). The presence of iron oxide is also evident (Plate 5.1f, g).

Interpretation: The SM facies occurring nearly at regular intervals in the Sukhbhadar Formation suggest cyclicity in a deposition. The lower contact of each layer is gradational with GSH facies (Plate 5.1, 5.2e), marking the periodic change in energy from low to calm condition, resulting in the accumulation of suspended fine silty mud for the short term. The subsequent partial dewatering of these muddy sediments resulted in subaqueous shrinkage cracks, giving three-dimensional polygonal shapes to the beds (Plate 5.1e) (McMahon *et al.* 2017). The cyclicity and gradation in the deposition of the facies suggest a variation in the energy condition from low to calm in the offshore lake environment.

5.2.1.1.4 Lithic Greywacke Facies (LGW)

Description: The facies is observed in the lower part of the Sukhbhadar Formation in a dug well near Ninama village (Plate 5.1h). It occurs above the lower basaltic flow as a 5m thick bed and a few centimeters thick beds at higher levels in the well section (Plate 5.1h). It is dark grey to black in colour. Petrographically, facies comprise rock fragments of volcanic origin and quartz grains (Plate 5.1i). Rock fragments are larger in size as compared to sand-size quartz grains and polygenetic in nature, mostly of fine grain basalts (Plate 5.1i, j) with intraformational (Plate 5.1j) rock fragments. Groundmass occurs as a dark grey to black matrix (Plate 5.1i) and cement is either calcareous or ferruginous (Plate 5.1i, j). The LGW is texturally immature and highly diagenetically altered due to solution activity.

Interpretation: LGW is the bottom-most bed marking the beginning of the basin fill, mainly characterized by large-size polygenetic rock fragments and texturally immature quartz grains suggesting very short transportation of the sediments. The high-density current loaded with coarse-grained material has deposited sediments episodically in the lake. The volcanic

lithic fragments dominate compared to quartz in LGW which suggests partial mechanical weathering of the probable source area, the Deccan Traps. The occurrence of LGW at higher levels in the well section (Plate 5.1h) marks another short-term high-energy event that gave rise to a similar type of sediments.

5.2.1.2 Carbonate Lithofacies

5.2.1.2.1 Grey Black Limestone Facies (GBL)

Description: Grey-black limestone is up to 60 cm thick, massive, thinly to thickly bedded, hard and compact with rectangle joints (Plate 5.2a, b). Weathering on the surface gives a light yellow to white colour while the fresh surfaces are grey to dark grey in colour (Plate 5.2b, c). The dark grey black colour of the GBL is due to the presence of organic matter. This facies occur widespread in the basin and their thickness increases towards south-southeast, near Moti Lakhavad village. The facies is also well exposed on the right bank of the Sukhbhadar River near Ninama, Ninama hills, Moti Lakhavad and Shekhdod villages.

Mudstone microfacies:

The mudstone microfacies is characterized by pure orthochemical composition, mainly consisting of micrite, microspar with chert (Plate 5.2d), organic matter (Plate 5.2e), and iron oxide (Plate 5.2f). The chertification and ferruginization have occurred as result of replacement of calcitic materials due to diagenetic modification (Plate 5.2f). Minor amount of sand and silt-sized quartz grains are present (Plate 5.2f).

Interpretation: The deposition of the carbonate suggests high salinity and a high rate of evaporation and restricted fine grain clastic supply. A plausible condition is developed for the precipitation of the carbonates in the entire basin due to its shallowing and has restricted the water supply. Hence the relative salinity remains high throughout and allows the precipitation of the fine carbonates.

5.2.1.2.2 Cherty Limestone Facies (CL)

Description: This facies is compact, hard and thinly bedded. It is yellow to buff coloured (Plate 5.3a) with the presence of light-coloured chert nodules. The weathered surface of the facies appears grey to black in colour (Plate 5.3 a, b, c). They occur as thin (up to 5cm) beds. The thickness of the beds is highly variable. It is observed in Ninama hill, Sukhbhadar River, Moti Lakhavad and Motamatra villages. The CL facies exhibit three microfacies.

Plate 5.2. a. Grey black limestone (GBL) facies from the Moti Lakhavad village showing jointed nature, exposed above the Deccan traps. b. Relics of a thin bed of highly jointed and weathered GBL at Sukhbhadar river, Ninama village. c. Large bouldery GBL at the top of Ninama hill, Ninama village. Photomicrographs of mudstone microfacies. d. Sparitization and chertification in the groundmass. e. Organic matter and f. Chert, Silt-sized quartz grains and iron oxide, (Ms- Microspar, Om- Organic matter, Qz- Quartz, Ch-Chert, Io- Iron oxide; Scale- hammer length- 33cm, ruler length- 30cm).

I. Peloidal wackestone-packstone microfacies:

The peloidal wackestone-packstone consists of micritic pellets, a few bioclasts, micrite and replacement by micro- and cryptocrystalline silica, microspar, pyrite and iron oxide (Plate 5.3d, e). The pellets are of various sizes ranging from 0.1 mm to 2.0 mm (Plate 5.2f). The centre of the pellets is recrystallized to microspar and/or silica while the peripheries are micritic in

nature (Plate 5.3f). A few spheres of free-floating calcareous algae are replaced by chert and iron oxide (Plate 5.3d). Elongated, broken algal filaments are also replaced by framboidal pyrite (Plate 5.3e, f).

II. Bioclastic bindstone microfacies:

It consists of ostracod and cladoceran branchiopods (arthropod) shell fragments (Plate 5.3g). The bioclast, pellets and quartz grains are bounded by algal mats which form the organic and micritic beige to dark brown-coloured laminae (Plate 5.3g, h, i, j). The opaque minerals (framboidal pyrite and iron oxide) and crypto-micro crystalline quartz also occur due to replacement. Muddy pellets are also modified to microspars (Plate 5.3i).

III. Cone-in-cone calcitic microfacies:

This microfacies is characterized by the presence of chevron bands of fibrous sparry calcite which are stacked to form a cone-in-cone structure (Plate 5.3k). The upward and downward growth of calcite (Plate 5.3k) gives the appearance of wavy laminations made of organic matter and micrite. The thickness of micro laminae is variable. Thick lenses of organic matter (Plate 5.3k) also occur between the fibrous calcitic structures.

Interpretation: This facies consists of various types of allochems including bioclasts of ostracods, cladocerans, and algae, with algal spheres. As their proportions are highly variable, the transitions from wackestone-packstone indicate fluctuating energy conditions during the deposition, probably in shallow lake environments. Preservation of diversified broken micro- and delicate biota might suggest their deposition took place in the reducing condition and the presence of abundant cladoceran fragments marks saline conditions (Cohen 1954). The bindstone (microbialites), wackestone, and packstone microfacies are commonly associated with shallow shore to nearshore settings of the lake (Reading 2009; Flügel 2010).

5.2.1.2.3 Marlite Facies (ML)

Description: This lithofacies is blocky and massive in nature but laterally transforms into a thick-bedded form (Fig. 5.5a). The facies is dirty yellow to light orange in colour (Plate 5.4a, b). The argillaceous materials occur as a matrix, with few sand-size quartz grains. The iron oxide and high organic matter have also led to brown to grey-coloured shading. Its thickness varies from 0.1m to >1.0 m (Plate 5.4a, b). It is observed from Ninama hill, Sukhbhadar River, Motamatra and Shekhdod villages. Cladoceran bindstone microfacies described herein.

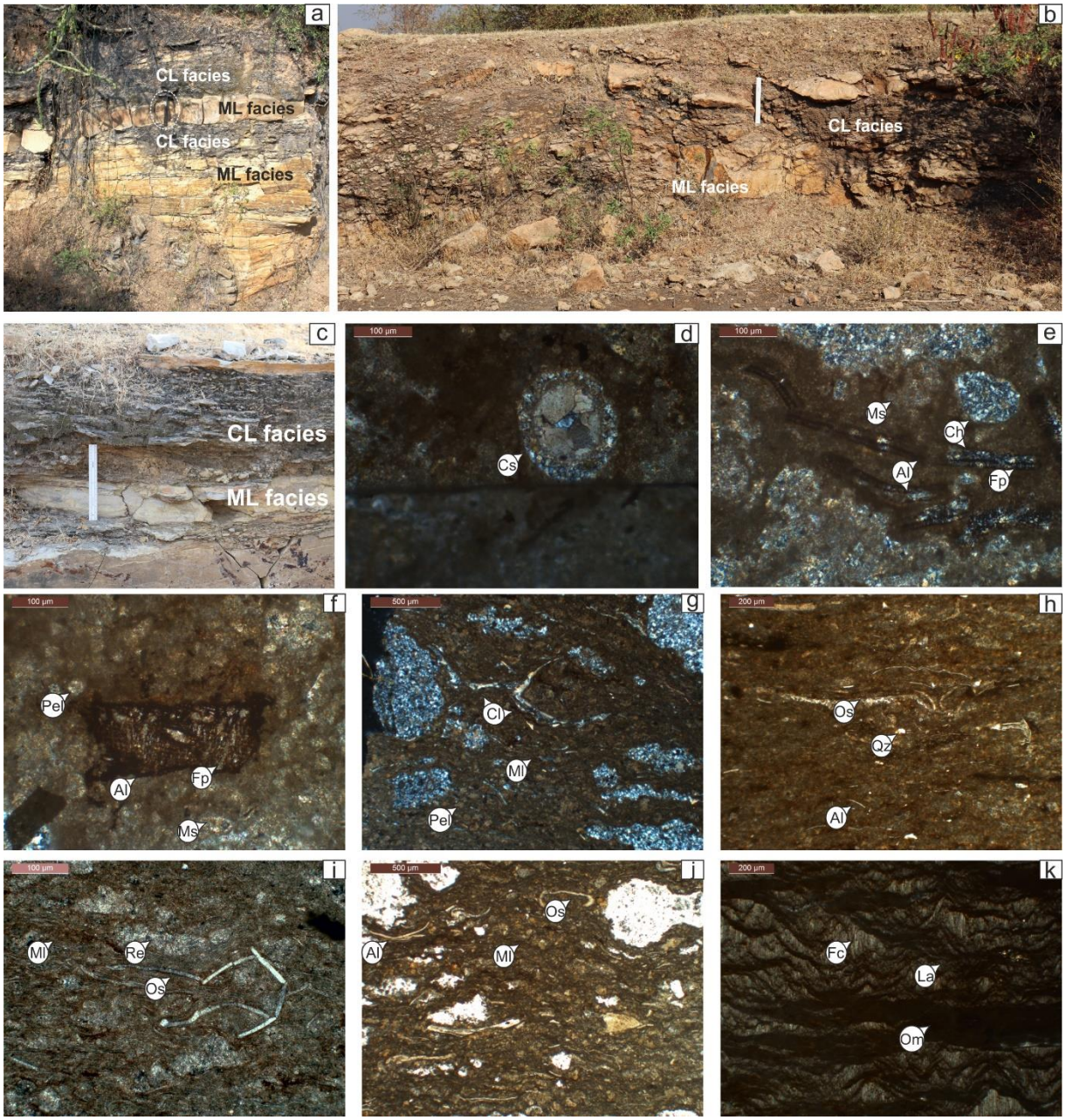

Plate 5.3 a. Cherty limestone (CL) facies exposed at the Ninama hill, intercalated with marlite facies (ML). b. Thinly bedded CL near Shekhdod village. c. Close-up of CL facies at the top of Sukhbhadar River. Photomicrographs of peloidal cherty wackestone microfacies. d. Calcareous sphere of floating calcareous algae, with replacement by chert and sparite e. Elongated dark algal filaments, partially replaced by framboidal pyrite and chert, as well as groundmass is also recrystallized to microspar and replaced by chert. f. Framboidal pyrite replacing the algae, pellet centres recrystallized into microspar. Bioclastic bindstone microfacies, g. Cladoceran shell fragments and pellets bounded together by microbial mats. Ostracod shell fragment. H. Algae with sit-size quartz grains. i. Micritic pellets modified to microspars. j. PPL view of bioclastic bindstone with ostracod shell fragments and algae. Cone in cone calcitic microfacies and k.

Cone in cone structures shows the growth of fibrous calcite which appeared as wavy laminae with organic matter, (Cs- Calcareous sphere, Ch- chert, Al- Algae, Fp- Framboidal pyrite, Pel- Pellet, Cl- Cladoceran, Os- Ostracod fragments, Fc- Fibrous calcite, La- Laminae Re - Recrystallized micrite, Ms- Microspar, Ml- Microbial laminations; Scale- hammer length- 33cm, ruler length- 30cm).

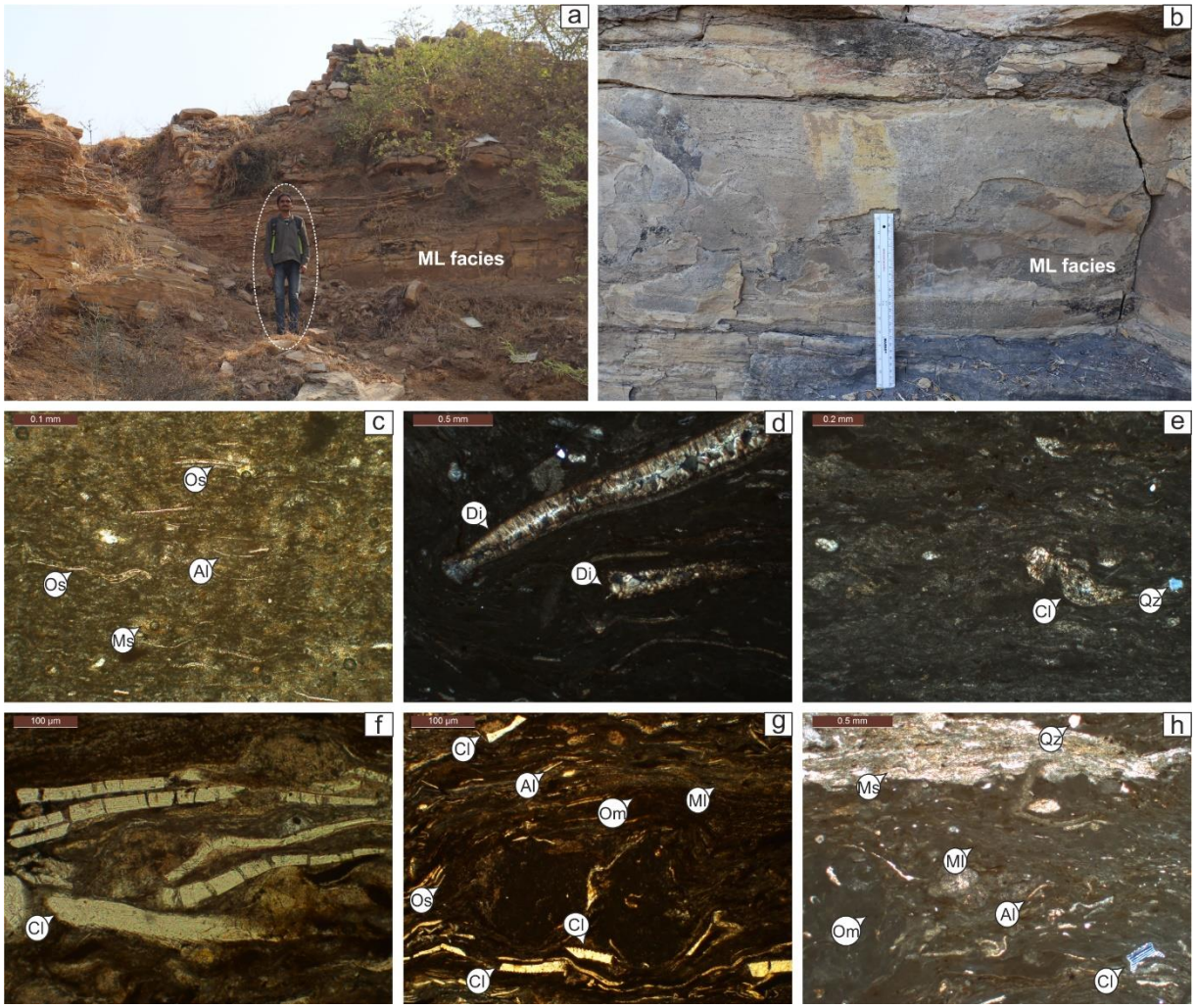

Plate 5.4 a. Exposures of the marlite facies (ML) near Ninama village and b. Thick bedded ML facies. Photomicrographs of cladoceran bindstone microfacies. c. Algae, ostracod shell fragments and microspar. d. Elongated diatoms in the laminated organic matrix e. Cladoceran shell fragments in the algal mats. f. Prefer oriented cladoceran appendages and their fragments. g. Algal filaments, cladoceran and ostracod fragments in well-laminated algal mats. h. Wavy-oriented organic matter and microspar bound with pellets and quartz, (Os- Ostracod fragments, Ms- Microspar, Al- Algae, Di- Diatoms, Cl- Cladoceran, Qz- Quartz, Om- Organic matter, Ml- Microbial laminations; Scale- person height- 175cm, ruler length- 30cm).

Cladoceran bindstone microfacies:

It is a finely laminated bindstone (microbialite) dominated by cladoceran fragments (Plate 5.4c, e, f, g), which are arranged parallel to subparallel with the algal bands (Plate 5.4c, f, g, h). The proportion of these bioclasts is persistent laterally and microfacies is also characterized by ostracod shells (Plate 5.4c, g), diatoms (Plate 5.4d), algae (Plate 5.4c, g, h), in broken forms (Plate 5.4d, e, f). It also consists of microspar, iron oxide and a minor amount of pyrite.

Interpretation: This facies consists of argillaceous sediments and bioclasts bounded within algal laminae, suggesting periodic growth of the algae. The alternating algal laminae and broken bioclasts indicate cyclic changes in energy conditions in the lacustrine environment. The presence of broken cladocerans with ostracods and diatoms in the marlite facies suggests carbonate-prone shore to nearshore setting (Cohen 1954; Reading 2009; Flügel 2010) in the continental realm.

5.2.2 CHOTILA BASIN

The facies analysis of the 27 m thick Chotila Basin sequence of Rangpar Formation, Chotila Chert and Bamanbor Formation has resulted in eight lithofacies belonging to clastic and biochemical sedimentary rocks (Table 5.2, Fig. 5.2).

5.2.2.1 Clastic Lithofacies

5.2.2.1.1 Fossiliferous Shaly Sandstone Facies (FSS)

Description: FSS lithofacies is characterized by shaly sandstone. The facies is fine-grained, grey to yellowish in colour and compact but highly indurated (Plate 5.5a). It is thinly to thickly bedded, with shaly contacts giving it fissility (Plate 5.5b, c). It is fossiliferous and contains mega shells of the mollusc including the bivalve and gastropods (Plate 5.5b) (discussed in Chapter 6) and vertebrate remains like fish (Borkar 1973, 1975, 1984). It only occurs in Bamanbor Formation and is exposed in Bamanbor Road Section (Plate 5.5e). It is observed in association with clay shale (CS) facies and silty shale (SS) facies (Plate 5.5a). The thickness of facies ranges from 2 to 4m. Petrographically, the facies consist of fine to medium, subrounded to subangular, moderately sorted monocrystalline – polycrystalline quartz in the calcareous and ferruginous cement (Plate 5.5d, e). It is texturally immature and highly diagenetically altered

due to solution activity. The sandstone is petrographically identified as greywacke according to Dott's scheme of sandstone classification (Plate 5.5d, e).

Sr. No.	Lithofacies	Characteristic Features
1.	Fossiliferous Shaly Sandstone (FSS)	Fine-grained, grey to yellowish in colour and compact but highly indurated.
2.	Clay Shale (CS)	Characterised by argillaceous shale which is soft and crumbly in nature, and varies from dark grey to grey, red, and yellow in colour.
3.	Silty Shale (SS)	Silt dominated argillaceous shale.
4.	Mudstone (MS)	Compact, thinly bedded clastic mudstone, white to red in colour.
5.	Fossiliferous Silty Mudstone (FSM)	Blocky, yellowish to greyish white silty mudstone with planorbid gastropods.
6.	Massive Chert (MC)	Massive yellowish white chert
7.	Laminated Chert (LC)	Laminated, compact, hard, white to grey chert with pseudo-ripples, folds and fish fossils
8.	Black Chert (BC)	Blackish grey to dark black in colour, due to the baking effect on the chert by the underlying and/or overlying Deccan lava flows, compact and laminated

Table 5.2 Lithofacies and their characteristic features of the Chotila Basin.

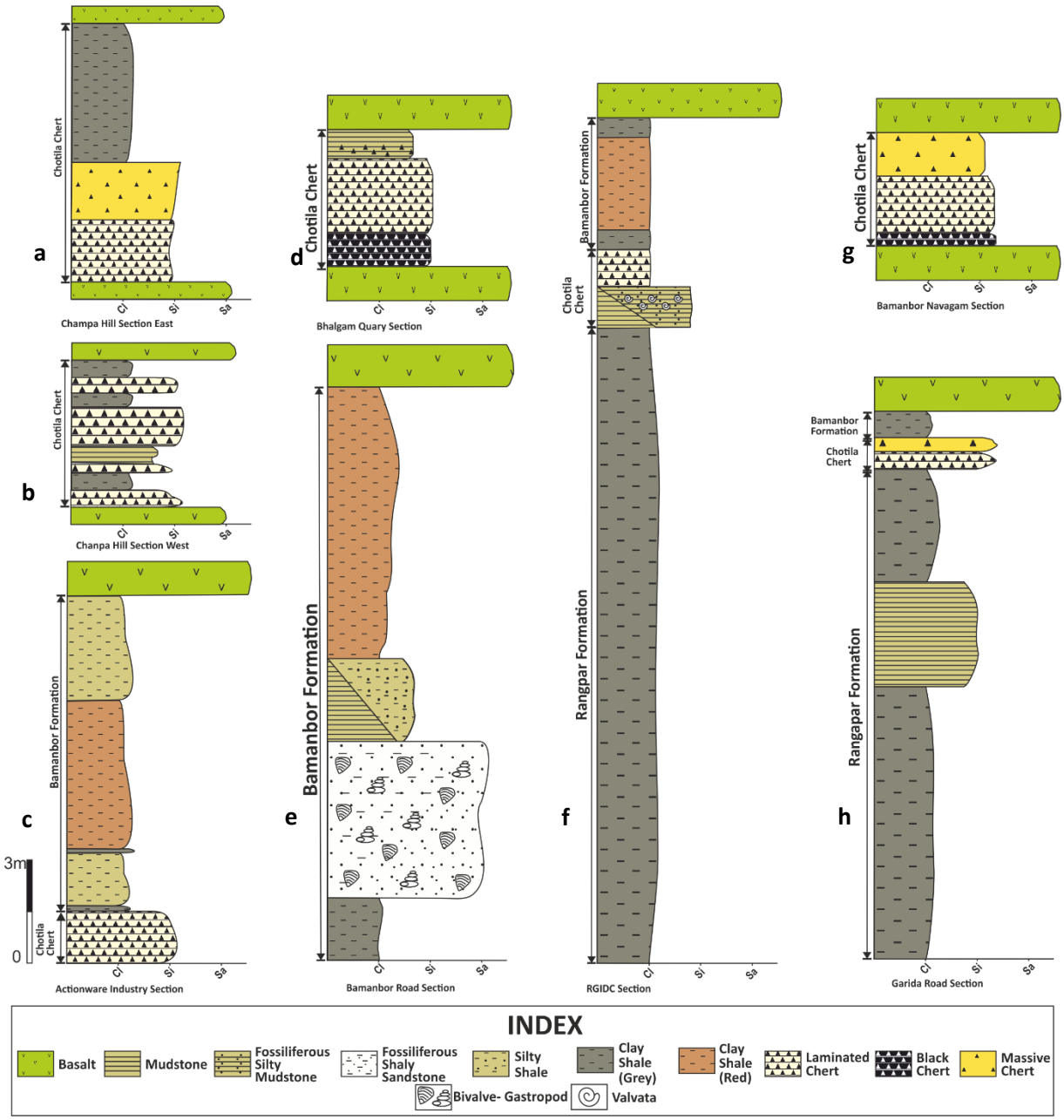

Fig. 5.2 Measured lithologs of the Chotila intertrappean sequence show the lithofacies distribution. a. Chanpa Hill Section East. b. Chanpa Hill Section West. c. Actionware Industry Section. d. Bhalgam Quarry Section. e. Bamanbor Road section. f. Rangpar GIDC Section (RGIDC). g. Bamanbor Navagam section and h. Garida Section.

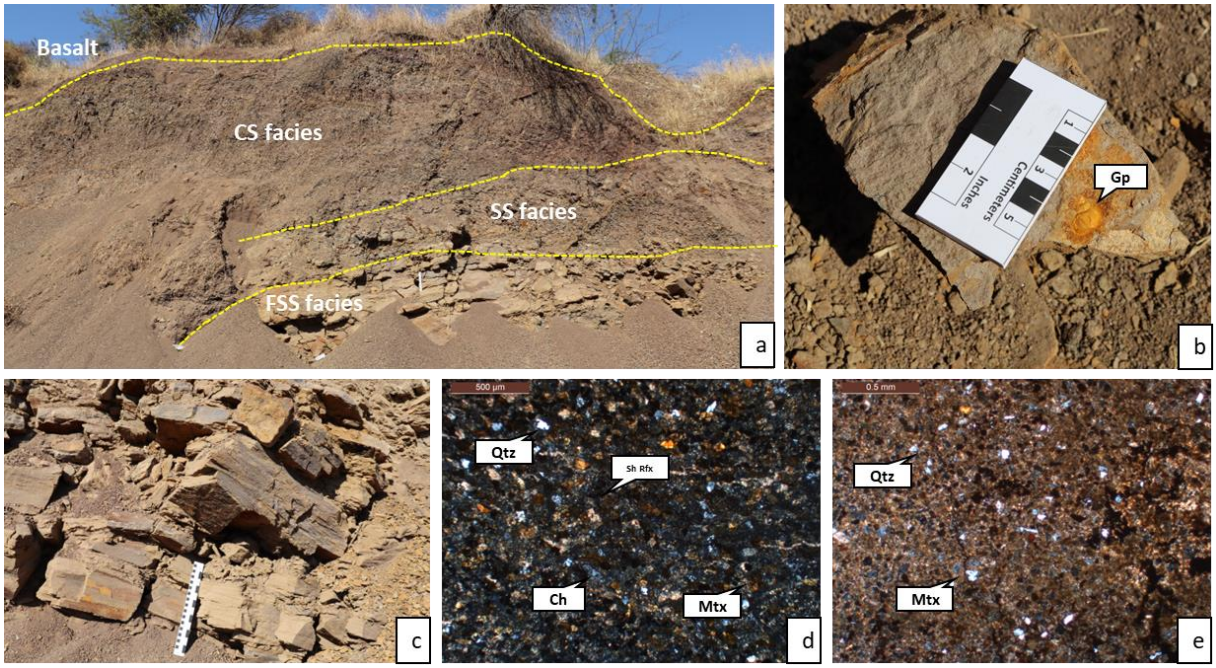

Plate 5.5 Fossiliferous shaly sandstone (FSS) lithofacies exposed at a. Bamanbor Road Section, overlain by silty shale facies (SS) and clay shale facies (CS) with b. Gastropod fossil, c. horizontal laminations in thin to thick beds of FSS. d. Photomicrographs of FSS d. and e. showing quartz, chert and muddy matrix embedded in a calcareous and ferruginous cement, (Gp- Gastropod, Qtz- Quartz, Ch- Chert, Sh rfx- Shale/mudstone lithic fragments, Mtx- Matrix).

Interpretation: This facies consists of fine to medium grained quartz, chert fragments and mudstone and shale clasts. The sediments contain significant amount of matrix, suggesting texturally sub-mature nature of the sandstone. The presence of sandstone is evident of short periodic high energy event in the basin. The facies suggest deposition in littoral or nearshore lake setting. The presence of bivalves and gastropods in the facies also suggests a habitable environment. The facies may also reflect the deposits of basin margins.

5.2.2.1.2 *Clay Shale Facies (CS)*

Description: The clay shale, CS facies is most frequently occurring and dominate the intertrappeans of the Chotila area. The facies is characterised by high argillaceous content which is soft, crumbly, and varies from dark grey to grey, red, and yellow in colour (Plate 5.5a, 5.6 a-f, 5.7a, c). It is fissile in nature and occurs in all three formations, Bamanbor, Chotila Chert and Rangpar (Fig. 5.2). The thickness of the CS facies is highly variable, ranging from few cm's to more than 5m. It is exposed in Bamanbor Road Section, Rangpar GIDC, Garida Section, Chanpa Section, Redren Industry and Actionware Industry Section (Fig. 5.2, Plate 5.5a, 5.6 a-

f, 5.7a, c). It is commonly observed in association with massive chert, laminated chert, fossiliferous shaly sandstone, mudstone, and Fossiliferous silty mudstone.

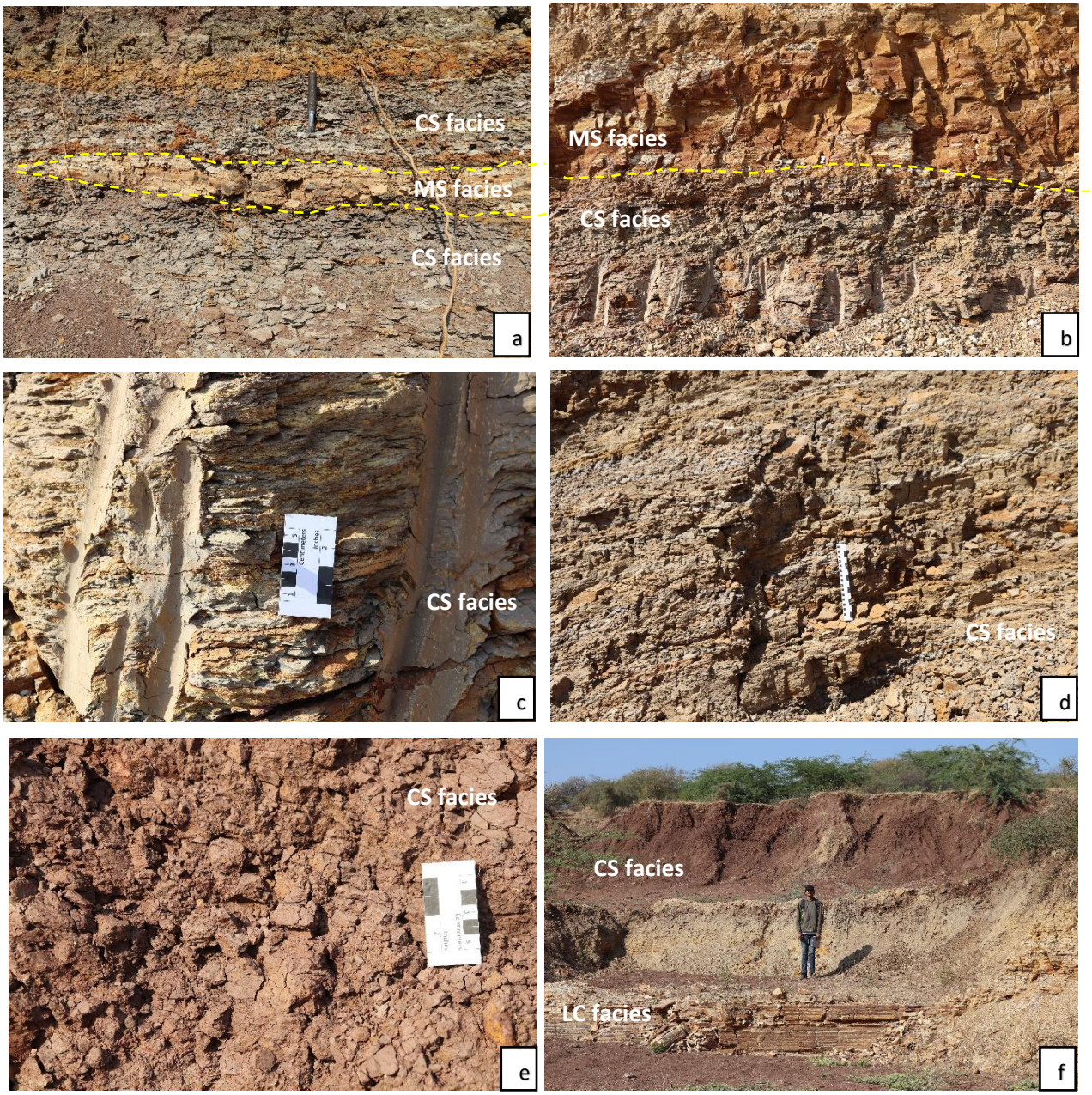

Plate 5.6 Clay shale facies (CS) of Rangpar Formation exposed at, a. RGIDC section, with intercalated mudstone (MS) facies, b. Garida Road Section where it is overlain by thick MS. CS facies of Bamanbor Formation, exposed at c. RGIDC section, showing characteristic fissility, d. Bamanbor Road Section and e. Red CS facies at Actionware Industry section and f. CS facies overlying laminated chert (LC) facies.

Interpretation: The clay shale facies suggest the deposition in calm conditions. The very fine-grained argillaceous nature of the sediments are reflecting quieter and deep lacustrine parts

of the lake, possibly suggesting the profundal zone (Wetzel, 2001). It also indicates that the basin received nearly no coarse terrigenous sediments. The infrequent massive and laminated occurrences are also typical of basin centre. The association of CS facies with FSS, SS, MC and LC facies suggests their interfingering with the marginal deposits as well as changes in the coarse clastic input periodically (Reading and Collinson, 1996).

5.2.2.1.3 Silty Shale Facies (SS)

Description: The silty shale facies is characterised by silt dominated argillaceous shale, massive to laminated and with moderate fissility (Plate 5.7). The CS facies shows lateral and vertical variations into SS facies locally. It occurs in all three formations and the thickness varies in few cm's.

Interpretation: The deposition of SS facies suggests periodic increase in fine to medium clastic input in the basin with continuous settling of clay. It is reflected by the pinching of the beds laterally and vertically. As the facies are patchy in nature, the periodic event of moderate energy is suggested.

5.2.2.1.4 Mudstone Facies (MS)

Description: The mudstone facies (MS) is characterised by the presence of thickly bedded clastic mudstone (Plate 5.7 b, c, d, e). It is compact and varies from white to red in colour. It occurs in Bamanbor Formation and Chotila Chert. The facies occur intimately with CS and LC facies. The thickness of the facies varies from 30 cm to 1-2 m. Petrographically it consists of an argillaceous matrix with clasts of mudstone and few rare quartz grains (Plate 5.10 a).

Interpretation: Massive to horizontally laminated mudstones dominate the axial zone of the lake system (Reading and Collinson 1996). The facies development suggests suspension materials are settling dominantly likely to be in standing water in the deeper parts of the lake. The intercalation with LC facies indicates periodic interruption in the chert precipitation due to high clastic input in the lake.

5.2.2.1.5 Fossiliferous Silty Mudstone Facies (FSM)

Description: The fossiliferous silty mudstone, FSM facies is poorly fissile, yellowish to greyish white, silty mudstone (Plate 5.8a). It contains abundant fossil remains of *Valvata* and other planorbid gastropods (Plate 5.8b). The thickness of this facies is 15 to 20cm.

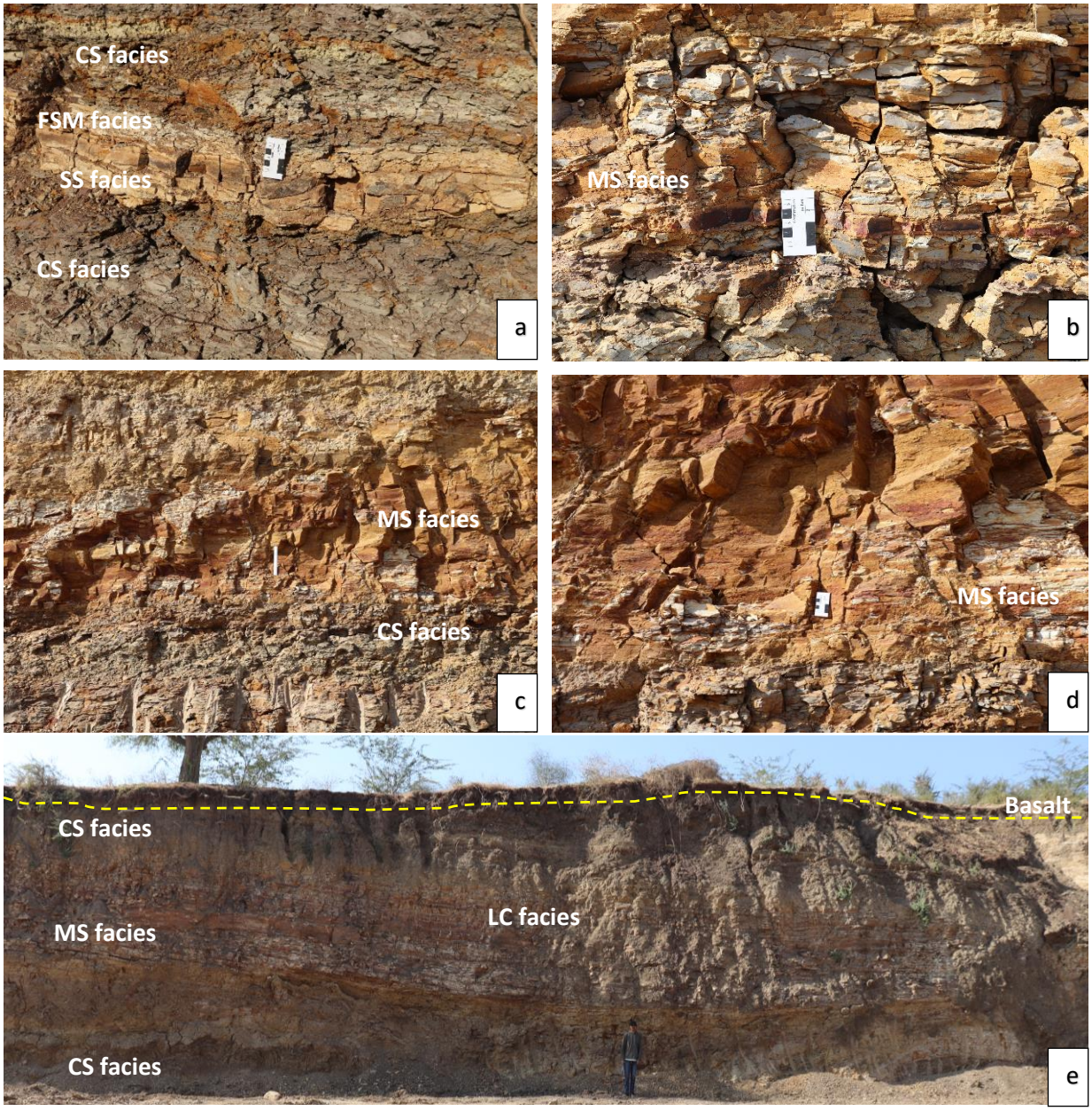

Plate 5.7 a. Silty shale facies (SS) and fossiliferous silty mudstone facies (FSM) intercalated between CS facies exposed at Rangpar GIDC section. Mudstone Lithofacies (MS) exposed at b. Rangpar GIDC Section, c. Bhalgam Quarry Section d. Garida Road Section, showing d. massive, thickly bedded nature and intercalation with CS facies and e. CS, MS and LC facies of Rangpar Formation, Chotila Chert and Bamanbor Formation.

Interpretation: FSM facies is locally developed and is characterised coarsely fissile and can easily crumble down in to small fragments. It is consisting of abundant fresh water gastropod species like *Valvata* with planorbid indicate deposition of the sediments took place in calm oxic conditions.

5.2.2.2 Biochemical Lithofacies

5.2.2.2.1 Laminated Chert Facies (LC)

Description: The facies is a laminated, compact, hard and white to grey chert. It shows characteristic laminations and alternate dark and light-coloured bands (Plate 5.9a). It occurs as both laminated and bedded, also at times intercalated with CS facies and MS facies (Plate 5.9 b, c). The facies is fossiliferous in nature, with fish remains are reported (Plate 5.9 d) (Borkar 1984; Arratia et al. 2004). The thickness of this facies ranges from 30 cm to 2-3m in various sections of Chotila Basin (Fig. 5.2, Plate 5.9 a-c). The facies show characteristic laminations with compactional structures like folding (Plate 5.9b), pseudo-ripples (Plate 5.9e), etc. formed due to the discordant and concordant lava flows. Petrographically, the facies show characteristic alternate bands of micro and crypto- crystalline silica with iron oxide and very rare quartz grains (Plate 5.10 b-f). The light and dark laminae insinuate the presence of alternate bands of micro crystalline quartz and cryptocrystalline quartz and the later can be mixed with detrital carbonaceous matter with microlaminae, which are the remnants of the microbial mats. Microfolds are also evident in the petrographic studies (Plate 5.9f).

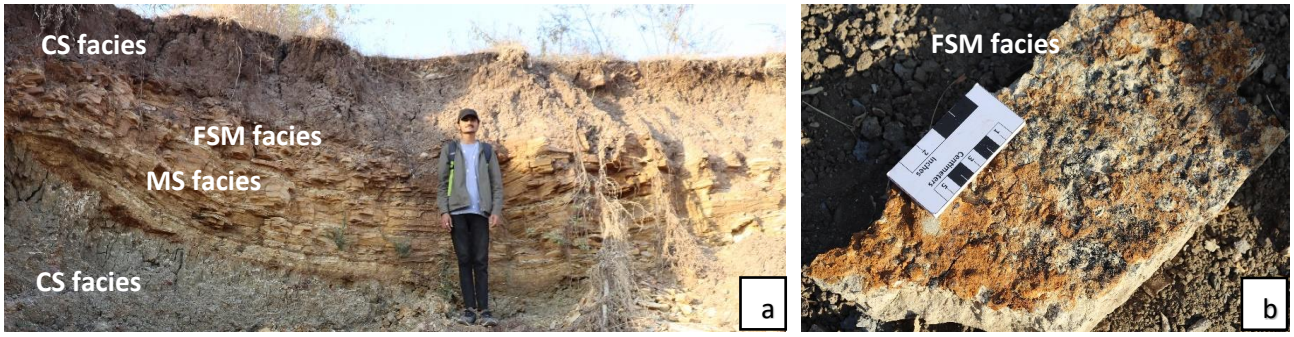

Plate 5.8 a. Fossiliferous silty mudstone facies (FSM) exposed at Rangapar GIDC Section and b. *Valvata* and various gastropods embedded in FSM.

Interpretation: The extensive precipitation of chert in the lake is thought to be formed by both biological as well as chemically processes. A direct precipitation of the chert in the basin from a silica rich alkaline lake, is probable. The intercalation with CS and MS facies shows occasional interruption due to settling of fine argillaceous clastics in quiet lake waters. The alternation in the laminae may imply destruction and reconstruction of lake stratification (Chough et al. 1996). The biological origin of the chert due to decomposition of algal organic matter lowered the pH of sediment pore waters and has caused silica precipitation (Kuma et al. 2019) is also considered in the study.

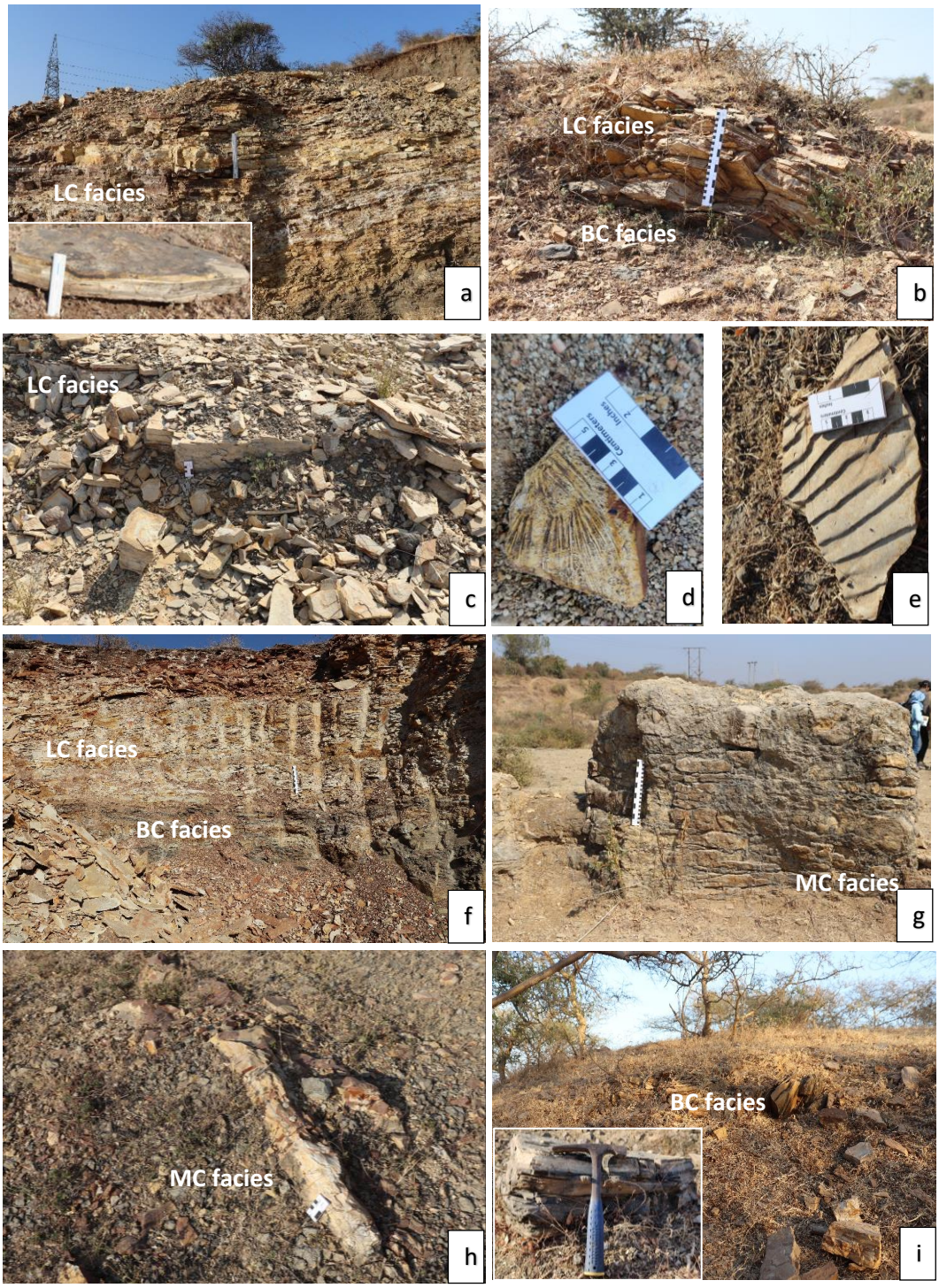

Plate 5.9 Laminated Chert Lithofacies (LC) exposed at a. Chanpa Hill Section East, with a closeup of LC (inset). b. Tilted and folded LC facies at Bamanbor Navagam Section. c. Chanpa Section, d. Vertebrate fossil (Fish Fin) in LC facies. e. Pseudo ripples in LC facies. f. Bhalgam Quarry Section showing LC and black chert facies. Massive Chert Lithofacies (MC) exposed. g. Bamanbor Navagam Section, h. Chanpa Hill Section East and i. Black Chert lithofacies (BC) exposed at Vasundhara Hill Section (close-up in inset).

5.2.2.2.2 Massive Chert Facies (MC)

Description: The Massive Chert facies occur as massive yellowish to white chert (Plate 5.9g). It is nearly homogeneous in nature and composition (Plate 5.9g, h). The chert is highly compact and associated with LC facies. The thickness of this facies is ranges from 15 cm to 1m.

Interpretation: This facies is developed locally and devoid of bedding planes. It is considered as lateral facies variation due to depositional parameters like in absence of current energy allow to precipitation of the silica continuously.

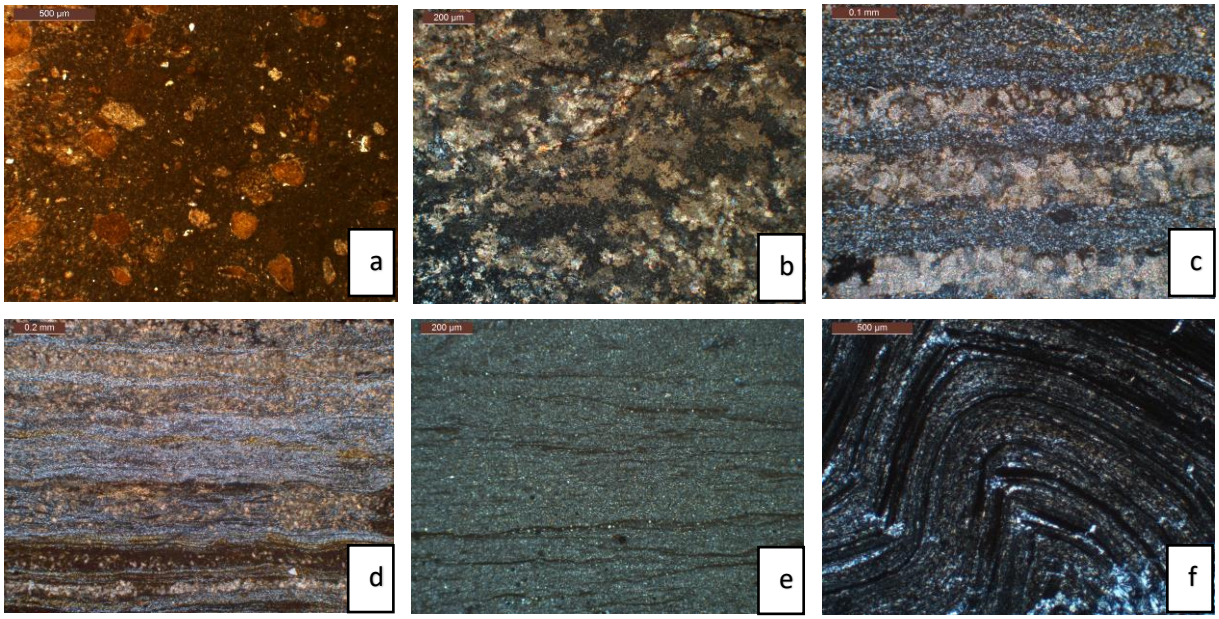

Plate 5.10 Photomicrographs of a. Mudstone facies. b, c and d. Laminated Chert Lithofacies showing alternate bands of microcrystalline and cryptocrystalline silica with dark bands of organic matter and iron oxide. e. thickly laminated chert facies with discontinuous laminae and dominated by microcrystalline quartz. f. Black chert facies with microfolds.

5.2.2.2.3 Black Chert Facies (BC)

Description: The Black Chert, BC lithofacies are blackish grey to dark black in colour. The chert is compact and laminated (Plate 5.9f, i (inset), Plate 5.10 f). This lithofacies is exposed in Bhalgam Quarry Section, Bamanbor Navagam Road Section and Vasundhara Hill Section. The thickness of this facies varies from few 30 cm to 1m. In Bamanbor Navagam Road Section the chert is in contact with Deccan basalts and upper boundary is in contact with LC facies. In Vasundhara Hill Section-1 lower boundary of this chert is in contact with deccan basalts and upper boundary is in contact with Chert (CR) of the same formation.

Interpretation: Black chert facies is also locally developed and distinguished based on their coloured characteristics. It is formed due to the baking effect of underlying and/or overlying Deccan lava flows when it come with contact, the chert is heated with high temperature cause primarily coloured alteration without hampering the mineral composition and their bedding properties.

5.3 GEOCHEMISTRY

The understanding of provenance, weathering rates, paleoclimate indicators, and the geological evolution of source areas are pivotal in deriving comprehensive insights into depositional settings (Ref). Petrographic analytical methods have traditionally served as fundamental approaches in unraveling these aspects, providing significant clues towards the tectonic context of the depositional basin (Grout, 1925; Goldschmidt, 1954; Keith and Bystron, 1959; Keith and Degens, 1959; Ernst, 1970). Over time, the application of advanced geochemical techniques has expanded the horizons of sedimentological investigations, enhancing the robustness and confidence in the findings (Nesbitt et al., 1980; Bhatia, 1981; Bhatia and Crook, 1986; Suttner and Dutta, 1986; Varma et al., 1991; McLennan et al., 1993; Fralic and Kronberg, 1997; Verma and Armstong-Altrin, 2013).

Geochemical analyses are pivotal in determining the distribution of major, minor, and trace elements within sediments, serving as indicators of provenance, weathering processes, and the tectonic setting of the depositional basin (Middleton, 1960; Piper, 1974; Bhatia, 1983; Cox and Lowe, 1995). The relationship between element occurrence and abundance reveals insights into various geological environments, with geochemical investigations offering advantages in their applicability to sediments of diverse grain sizes and mineralogically altered rocks. The chemical composition of sedimentary rocks summarizes their evolutionary history, making geochemical data invaluable for understanding sediment recycling and providing details not easily discernible through petrographic investigations (Hiscott, 1984; Garver et al., 1996). Certain trace elements like Ni, Cr, Co, and V hold significance in discriminating provenance and tectonic settings, while some Rare Earth Elements (REEs), owing to their relative immobility during sedimentary processes, play a crucial role in provenance discrimination (Holland, 1978; Taylor and McLennan, 1985). The distribution of elements within sediments is influenced by source rock composition, weathering, transportation processes, depositional conditions, tectonic events, and diagenetic processes (Spencer et al., 1968; Fralick and

Kronberg, 1997; Sawyer, 1986). Additionally, hydrothermal alteration, metamorphism, and elemental mobility further impact sediment rock chemistry (Hayashi et al., 1997).

The instrument SPECTRO XEPOS HE XRF ('HE' stands for 'Heavy Elements') was used which can reliably quantify heavy elements in ppm ranges (Abuhani et al. 2014; Matson et al. 2015) due to a versatile excitation source. It has a 50-watt end-window tube that is exceptionally steady, with up to eight polarisation and secondary targets, exceptional sensitivity and accuracy to analyse medium and heavy elements. Major oxides weight % determined in samples are SiO2, TiO2, Al2O3, Fe2O3, MnO, MgO, CaO, Na2O, K2O, and P2O5 (Table 5.3). Minor and trace elements detected in geological samples better than 10% include Al, Ba, Ca, Co, Cr, Cs, Cu, Fe, Ga, Hf, K, Mg, Nb, Ni, Pb, Rb, Sc, Sr, Th, Ti, U, V, Y, Zn and Zr (Table 5.3). X-ray Fluorescence Spectrometry is an established multi-element analysis technique utilized for bulk sample identification and quantitative estimation of almost any element from Boron to Uranium at concentrations between 1ppm to 100%. The primary benefits of this technique include the need for a minimal sample size, rapidity, and high precision. Consequently, XRF spectrometry is regarded as one of the most versatile and extensively employed analytical methods in geochemical analysis.

Various geochemical proxies using elemental ratios like Ca/(Ca+Fe) and Sr/Ba for salinity (Armstrong-altrin *et al.* 2015; Wei and Algeo 2020), V/(V+Ni) (Lewan and Maynard 1982; Lewan 1984; Hatch and Leventhal 1992; Jones and Manning 1994) and V/Cr for paleoredox conditions (Jones and Manning 1994), and Fe/(Ca+Mg) for water depth (Restituito 1987; Chen *et al.* 2016), were used to determine the variations in the depositional environment.

The salinity of both modern and paleolakes can be measured using the ratios of Sr/Ba and Ca/(Ca + Fe), which has a positive correlation with salinity (Armstrong-altrin *et al.* 2015; Wei and Algeo 2020). Because Sr is relatively enriched in salty water while Ba is more enriched in fresh water, the ratio of Sr to Ba can be used as a salinity index for carbonate deprived rock types, in the present case SH and SM facies (Table 2) (Wei and Algeo 2020; Gu *et al.* 2022).

The redox-sensitive elemental ratio of V/(V+Ni) is used to infer the paleoredox conditions as Vanadium gets enriched in a reducing environment while Nickel gets enriched in oxidizing conditions (Lewan and Maynard 1982; Lewan 1984; Hatch and Leventhal 1992). V/(V+Ni) value >0.54 indicates anoxic conditions, 0.46–0.6 shows dysoxic conditions, and <0.46 shows oxic environments (Jones and Manning 1994). The paleoredox conditions

determined by V/Cr, if <2 indicates oxic conditions, 2 < V/Cr <4.5 indicates dysoxic conditions and >4.5 indicates suboxic to anoxic conditions (Jones and Manning 1994).

The corresponding lithofacies depositional water depth is estimated using Fe/(Ca+Mg) ratios (Restituito 1987). Fe is enriched in terrigenous rocks while Ca and Mg are enriched in carbonates and mudrocks, with high values of Fe/(Ca+Mg), which can indicate deep waters of the paleolake during deposition (Restituito 1987; Chen *et al.* 2016).

Volcanic proxies, such as Na/K and K/(Fe+Mg) which represents the balance between detrital and volcanic input (Sageman and Lyons 2005; Pujol *et al.* 2006; Keller *et al.* 2012) were also used. The values of Ti/Al are indicative of the relative amount of detrital influx during the deposition and differentiate the source of sediments from felsic, intermediate and mafic (Hayashi *et al.* 1997; He *et al.* 2017). The influence of volcanism is evaluated based on Ti/Al, Na/K and K/(Fe+Mg) (Sageman and Lyons 2005) ratios which evaluate detrital influx, and volcanogenic input during the deposition (Fantasia *et al.* 2016). Titanium has very low mobility under almost all environmental conditions, owing primarily to the high stability of the insoluble oxide of TiO_2 (Brookins, 1988). Aluminum, Silicon and Zirconium are also used frequently to measure the detrital influx due to their immobile nature during diagenetic processes (Algeo and Maynard 2004).

The Chemical Index of Alteration (CIA-K), a weathering index, is used to assess the amount of chemical weathering due to associated climatic changes (Sheldon *et al.* 2002). This index does not include potassium (K) because diagenetic processes can yield elevated concentrations of K (Sheldon *et al.* 2002; Adams *et al.* 2011). The calculation is based on molar proportions using Nesbitt and Young (1982, 1989),

$$CIA\text{-}K = Al_2O_3 \times 100/(Al_2O_3 + CaO^* + Na_2O),$$

where CaO* is the CaO in silicate minerals only, so CaO correction was applied due to the presence of carbonates, and we assume that CaO* is equivalent to Na_2O as the CaO is higher than Na_2O after correction (McLennan *et al.* 1993). To determine whether the severity of weathering is related to the quantity of precipitation, quantitative Mean Annual Precipitation (MAP) was also calculated using CIA-K values.

$$\text{MAP (millimeters/year)} = 221exp^{0.0197CIA-K}$$

(Sheldon *et al.* 2002; Sheldon and Tabor 2009)

5.3.1 NINAMA BASIN

A total of 21 samples were analyzed, 3 of GBL facies, 6 of CL and ML facies, 8 of SH facies and 1 of SM facies, 3 of LGW facies. Average concentration of selected major oxides, minor and trace elements of the different lithofacies of Ninama Basin are mentioned below which are used to interpret the environment of deposition. Remaining data of the minor and trace elements of the each lithofacies are also tabulated (Table 5.3) that gives full length of information.

The LGW facies consists of SiO_2 (avg. 40.26 wt.%), CaO (avg. 13.54 wt.%), Fe_2O_3 (avg. 7.47 wt.%), Al_2O_3 (avg. 9.54 wt.%), MgO (avg. 6.67 wt.%), Ti (avg. 1.73 wt.%), Na_2O (1.44 wt.%), Mn (avg. 0.143 wt.%), Sr (avg. 280.33 ppm), Zr (avg. 315.1 ppm), and Rb (avg. 27.9 ppm). SH and SM facies consists of SiO_2 (avg. 36.2 wt.%), CaO (avg. 10.92 wt.%), Fe_2O_3 (avg. 15.58 wt.%), Al_2O_3 (avg. 15.91 wt.%), MgO (avg. 2.55 wt.%), TiO_2 (avg. 2.14 wt.%), Na_2O (1.61 wt.%), MnO (avg. 0.33 wt.%), SrO (avg. 317.05 ppm), Zr (avg. 448.9 ppm) and Rb (avg. 59.81 ppm). CL and ML facies consists of SiO_2 (avg. 32.21 wt.%), CaO (avg. 32.58 wt.%), Fe_2O_3 (avg. 3.65 wt.%), Al_2O_3 (avg. 4.43 wt.%), MgO (avg. 3.05 wt.%), TiO_2 (avg. 0.56 wt.%), Na_2O (avg. 0.77 wt.%), MnO (avg. 0.09 wt.%), SrO (avg. 377.35 ppm) Zr (avg. 124.9 ppm), and Rb (avg. 25.58 ppm). GBL facies consists of SiO_2 (avg. 20.076 wt.%), CaO (avg. 22.38 wt.%), Fe_2O_3 (avg. 3.01 wt.%), Al_2O_3 (avg. 7.57 wt.%), MgO (avg. 15.72 wt.%), TiO_2 (avg. 0.95 wt.%), Na_2O (avg. 1.26 wt.%), MnO (avg. 0.06 wt.%), SrO (avg. 290.96 ppm) Zr (avg. 207.9 ppm) and Rb (avg. 26.5 ppm). These elements are associated with minerals like quartz, calcite, dolomite, pyrite, hematite and clay minerals.

5.3.1.1 Paleosalinity

In the Ninama Basin, the ratio of Ca/(Ca+Fe) is 0.58 in LGW facies, 0.28 for SH and SM facies, 0.88 for CL and ML facies, and 0.85 for GBL facies (Table 5.3). The value of Sr/Ba is 0.69 in SH and SM facies. (Table 5.3). The Ca/Ca+Fe ratio of 0.8 corresponds to the saline water, ratios ranging from 0.4 to 0.8 indicates brackish water, and <0.4 indicates freshwater (He *et al.* 2017; Khan *et al.* 2023). The ratio of Ca/(Ca+Fe) is 0.58 for LGW facies suggests its deposition in brackish conditions and 0.88 for CL and ML facies, and 0.85 for GBL facies suggests deposition in saline conditions (Fig. 5.3). The SH and SM facies with 0.69 Sr/Ba ratio suggests deposition in saline water (Wei and Algeo 2020; Gu *et al.* 2022) while Ca/Ca+Fe of 0.28 suggests deposition in freshwater (He *et al.* 2017). Due to stratigraphic temporal evolution

of these elemental ratios which reflects the change in water paleosalinity from brackish water during the early short period to fresh-saline water, and dominantly saline water in the late stage of the lake which is consistent with paleoclimate change (He *et al.* 2017).

A decrease in the Ca/(Ca+Fe) initially from LGW to SH and SM, with a gradual increase in ratio of Ca/(Ca+Fe) from bottom to top during the deposition of CL and ML, and GBL facies (Fig. 5.3a, b) might have been caused by gradual depletion of lake level due to semi-arid climatic conditions (He *et al.* 2017). The Ca/(Ca+Fe) and Sr/Ba ratio changes frequently (Fig.), which indicates that the lake salinity in the study area is highly inconsistent probably due to the change in local environmental conditions, including sediment and water influx. The change in salinity, as depicted by varying elemental ratios (Fig. 5.3a), is also reflected by the lithofacies (Fig. 5.3a). The deposition of limestone lithofacies, such as ML, CL, and GBL facies, indicates higher salinity and the deposition of fine and coarse clastic lithofacies, SH, SM, and LGW facies, indicates low or fluctuating salinity (Anadon *et al.* 1991; Gallois *et al.* 2018).

5.3.1.2 Paleoredox conditions

In the Ninama Basin, the value of V/(V+Ni) for LGW facies is 0.57 (dysoxic), for SH and SM facies 0.93 (anoxic), for CL and ML facies averages 0.88 (anoxic) and GBL facies averages 0.91 (anoxic) (Table 5.3).

The values of V/Cr for the Ninama Basin are 1.56 (oxic) for LGW facies, 5.22 (anoxic) for SH and SM facies, 3.06 (dysoxic) for CL and ML facies and 1.86 (oxic to dysoxic) for GBL facies (Table 5.3).

The elemental ratios for both the paleoredox indicators, V/V+Ni and V/Cr show dissimilar results. This variation might have been caused due to local depositional parameters. Hence, their wide ranges are considered for each lithofacies, coupling the data of both analyses. Initially, LGW facies show the oxic-dysoxic conditions, gradually changing to anoxic in SH and SM, and ML and CL facies, and finally, to oxic to anoxic conditions during the deposition of GBL facies at the close of the Ninama Basin (Fig. 5.3 c, d).

5.3.1.3 Paleodepth

The average values of Fe/(Ca+Mg) are 0.82 for LGW facies, 2.26 for SH and SM facies, 0.13 for CL and ML facies and 0.14 for GBL facies (Table 5.3). These values indicate that paleodepth has controlled the sedimentation pattern in the basin. The values of LGW facies

indicate a moderate water depth during the deposition, where the topographic low provided the accommodation space for the accumulation of the coarse-grained sediments initially. The calculated average ratio increases for SH and SM facies suggesting deep water conditions, which aided in the deposition of the fine-grained clastic sediments. The average value of limestone lithofacies, CL and ML facies; and GBL facies is very low (Fig. 5.3e) and can be inferred as shallow water depths during their deposition. Their pervasive occurrence in the basin also envisages shallowing.

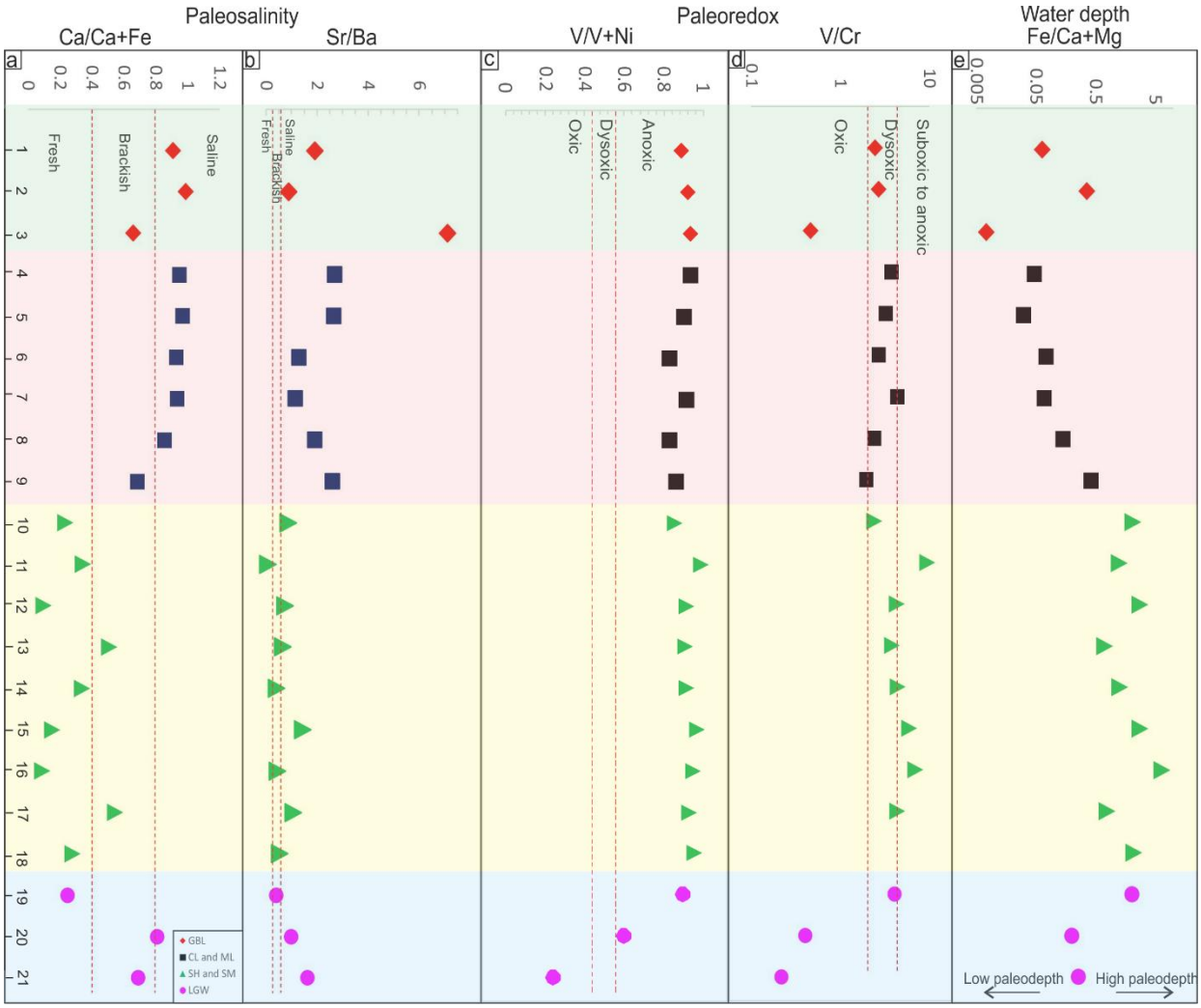

Fig. 5.3, Plot of the geochemical proxies for paleosalinity, a. Ca/(Ca+Fe), b. Sr/Ba; paleoredox c. V/V+Ni, d. V/Cr; paleodepth e. Fe/(Ca+Mg), of the Ninama Basin.

5.3.1.4 Paleoweathering and paleoclimatic conditions

The average value of Ti/Al for various lithofacies is 0.22 for LGW facies, 0.15 for SH and SM facies, 0.13 for CL and ML facies and 0.11 for GBL facies (Table 5.3). The high Ti/Al values are indicative of mafic composition of the host rocks and relatively high rate of detrital input in the basin. The SH, SM and LGW facies are closer to the Ti/Al values of Average Deccan Basalt Composition (ADBC) 0.19 (Fig. 5.14a), as given by Crocket and Paul (2004).

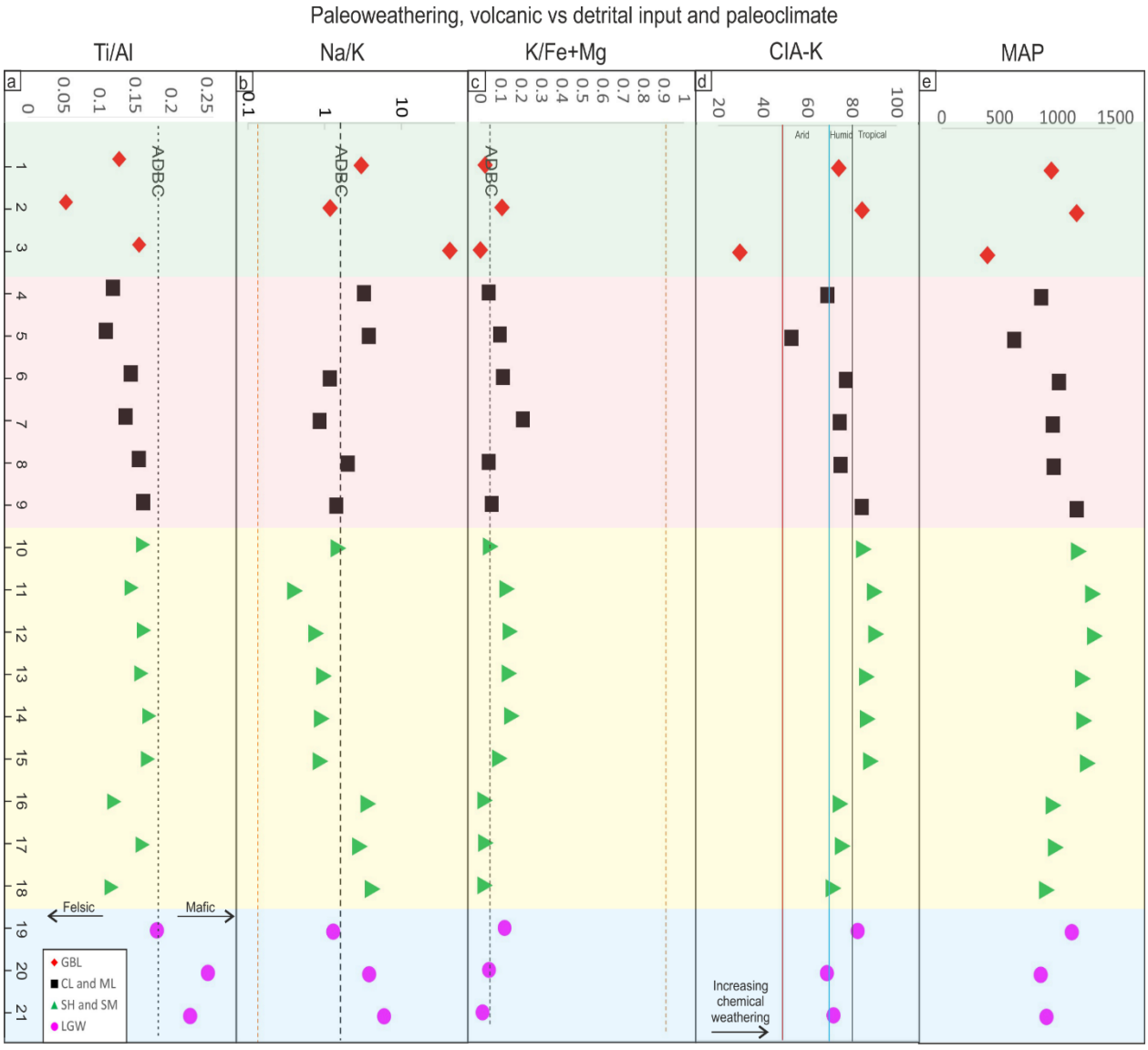

Fig. 5.4 Plot of the geochemical proxies for paleoweathering, volcanic vs detrital input and paleoclimate, a. Ti/Al, b. Na/K, c. K/Fe+Mg, d. Al/Ti, e. CIA-K, and f. MAP, of the Ninama Basin.

The CIA-K average value for LGW facies is 74.28%, SH and SM facies are 83.44%, for CL and ML facies are 72.12%, and for GBL facies is 62.66% (Fig. 5.4d). The CIA-K average values from bottom to the top suggest a change in climatic conditions from humid-tropical to semi-arid. The value of the LGW facies suggests a humid-tropical climate prone to chemical weathering which intensified during the deposition of the SH and SM facies. Further, the averages shows of the CL and ML facies decreases suggesting a moderately humid climate and chemical weathering and finally, GBL facies shows a relatively low average value, which suggests a semi-arid climate.

CIA-K values were also used to calculate the Mean Annual Precipitation (MAP) to understand the intensity of weathering linked to the quantity of precipitation. The MAP values average 1185 mm for SH and SM facies (Fig. 5.4e). The higher value of SH and SM facies is suggestive of relatively high precipitation (Fig. 5.4e). The average values are consistent with the current climate in western India, which is hot and semi-arid with nearly identical seasonal rainfall (Venkatesh *et al.* 2021).

Sample No.	NS/NL/1	NS/NL/2	NS/NL/3	NS/NL/4	NS/NL/5	NS/NL/6	NS/NL/7	NS/NL/8	NS/NL/9	NS/SF/10	NS/SF/11	NS/SF/12	NS/SF/13	NS/SF/14	NS/SF/15	NS/SF/16	NS/SF/17	NS/SF/18	NS/SF/19	NS/SF/20	NS/SF/21
Major Oxides																					
SiO_2	17.72	1.54	40.97	15.91	20.30	41.39	35.20	40.99	39.50	43.64	55.96	53.65	47.31	48.38	47.32	42.19	25.24	36.20	39.77	39.34	41.68
Al_2O_3	6.62	1.04	15.07	4.10	2.49	3.18	3.78	4.01	9.02	15.99	12.52	18.95	15.89	17.98	18.24	17.20	11.08	15.34	16.44	6.45	5.74
Fe_2O_3	2.39	0.39	6.25	2.13	1.48	2.53	2.53	4.08	9.15	16.17	10.35	8.02	6.69	7.80	12.69	30.92	21.17	28.89	10.14	5.33	6.96
MnO	0.03	0.03	0.10	0.04	0.08	0.11	0.09	0.11	0.10	0.15	0.03	0.04	0.04	0.11	0.09	0.25	0.84	1.45	0.11	0.20	0.12
MgO	16.74	23.98	6.45	5.93	2.02	1.51	1.47	5.22	2.17	3.20	3.21	2.36	2.92	2.41	2.67	1.92	2.01	2.33	1.94	4.69	13.37
CaO	22.98	32.37	11.79	39.27	45.72	32.21	35.06	23.73	19.52	4.85	5.33	0.84	6.76	3.93	2.23	3.00	25.00	10.92	3.27	22.15	15.21
Na_2O	1.17	1.23	1.39	0.92	1.11	0.47	0.65	0.68	0.84	1.39	0.67	1.09	1.22	1.33	1.19	2.88	1.76	3.03	1.74	1.47	1.14
K_2O	0.35	0.03	1.06	0.26	0.26	0.36	0.67	0.30	0.53	0.82	1.47	1.26	1.11	1.29	1.21	0.70	0.54	0.64	1.20	0.35	0.17
TiO_2	0.75	0.05	2.07	0.43	0.24	0.41	0.46	0.55	1.29	2.28	1.61	2.72	2.24	2.71	2.72	1.85	1.58	1.60	2.63	1.44	1.15
P_2O_5	0.27	0.10	0.26	0.35	0.40	0.35	0.40	0.15	0.30	0.21	0.23	0.24	0.24	0.25	0.29	1.76	1.40	2.10	0.24	0.33	0.23
Total	69.02	60.76	85.42	69.35	74.10	82.52	80.30	79.81	82.42	88.70	91.38	89.17	84.41	86.18	88.65	102.6	90.61	102.5	77.48	81.74	85.77
CIA-K	73.95	84.40	29.65	68.97	52.85	77.28	74.54	74.79	84.33	85.21	90.29	90.75	86.74	87.11	88.42	74.91	75.91	71.68	82.54	68.72	71.59
MAP	948.5	1165	396.3	860.0	625.9	1012.	959.7	964.3	1163	1184	1308	1320	1220	1229	1261	966.7	985.96	907.1	1123	855.79	905.54
Minor and Trace Elements																					
Al	35060	79760	5487	21720	13170	16850	19990	21220	47760	84630	66250	100300	84120	95190	96570	91050	58650	81200	87000	34120	30390
Ba	129.7	241.2	38.80	89.10	106.0	168.7	186.9	192.1	233.7	306.80	3841	261.80	290.80	515.50	193.80	373.20	463.70	691.00	524.90	315.90	121.20
Ca	164300	84240	231300	280700	326800	230200	250600	169600	139500	34650	38090	6029	48300	28080	15920	21430	178700	78020	23390	158300	108700
Co	< 3.0	< 1.8	< 7.3	< 3.0	< 3.0	< 3.0	< 2.3	< 0.3	< 5.3	< 4.2	< 4.1	< 6.4	10.90	11.50	14.80	18.20	39.00	27.50	< 0.7	35.00	25.20
Cr	31.20	66.10	53.10	47.00	58.00	54.00	50.60	58.30	106.70	111.70	88.50	47.50	46.40	46.90	38.70	25.40	31.50	28.10	47.20	774.30	683.00
Cs	19.70	< 1.0	4.60	9.50	11.90	13.30	13.90	12.10	10.30	15.50	17.80	14.10	11.70	12.30	7.20	4.80	8.90	4.80	9.60	10.70	6.90
Cu	21.20	32.90	2.60	10.70	6.50	9.40	14.80	16.40	32.30	54.60	36.20	49.60	45.80	39.20	60.80	40.60	36.60	30.50	46.30	40.60	39.90
Fe	16700	43740	2740	14920	10380	17720	17720	28530	63990	113100	72360	56060	46750	54530	88760	216300	148100	202000	70930	37300	48670
Ga	10.50	22.10	3.70	6.00	5.80	7.20	9.50	8.40	15.70	23.90	20.90	30.70	26.80	28.40	30.30	15.60	16.00	12.60	27.70	9.90	12.40

Hf	< 2.0	3.30	< 2.5	< 2.0	< 2.0	< 2.0	< 2.0	< 2.0	< 2.0	5.90	< 3.5	11.30	7.40	9.00	8.90	< 6.4	< 2.0	< 2.0	5.80	< 2.0	< 2.0
K	2903	8800	214	2123	2188	3002	5562	2519	4405	6817	12210	10450	9237	10730	10040	5779	4510	5340	9955	2864	1430
Mg	101000	38860	144600	35730	12170	9100	8870	31480	13100	19290	19360	14240	17590	14540	16110	11560	12120	14050	11690	28290	80620
Nb	20.00	51.70	1.30	9.80	6.60	10.70	12.40	15.20	35.40	62.60	41.60	76.30	65.20	74.20	67.70	38.50	37.20	33.30	72.40	21.00	17.50
Ni	9.80	12.60	< 2.0	12.10	20.10	29.80	20.00	27.70	32.30	44.70	9.80	18.60	17.60	18.00	6.40	8.80	9.70	7.00	22.20	208.6	468.9
Pb	6.20	13.10	3.40	8.60	7.70	7.30	7.90	6.90	9.90	15.80	18.90	17.00	16.30	17.60	14.50	12.80	10.80	9.00	17.90	10.20	4.10
Rb	23.80	53.50	2.30	17.50	17.40	25.90	40.10	21.40	31.20	50.80	73.20	90.40	72.50	71.30	80.20	35.10	35.20	29.60	66.50	11.60	5.60
Sc		41.00								24.50	33.10	16.90	22.50	20.20	27.10	25.20		57.00	12.90		
Sr	248.1	214.3	275.7	238.1	280.6	215.	211.6	365.0	604.2	264.5	247.1	194.2	189.8	208.6	279.1	167.6	490.9	371.1	206.8	308.5	195.8
Th	8.10	18.10	3.20	4.80	4.80	4.30	6.90	6.40	13.10	20.60	16.80	26.40	26.70	24.30	21.80	9.10	12.90	6.70	19.40	5.30	5.10
Ti	4483	12410	292	2597	1445	2436	2738	3299	7717	13670	9663	16320	13410	16210	16280	11070	9444	9559	15740	8608	6914
U	2.40	3.50	0.60	2.60	6.30	5.60	11.00	4.70	10.40	4.10	7.30	5.70	4.00	3.90	4.60	3.60	5.60	< 2.9	2.90	3.60	1.50
V	76.50	177.8	24.60	176.7	187.8	146.4	219.9	140.2	208.5	269.8	839.0	204.2	176.0	206.8	231.0	177.7	137.5	149.8	191.9	314.5	148.1
Y	14.20	42.50	< 0.5	6.40	4.90	7.30	7.80	12.30	29.90	53.60	42.90	59.00	55.50	56.80	60.40	85.00	133.1	86.60	60.20	15.40	11.90
Zn	35.60	94.70	7.40	22.00	20.80	34.80	33.20	39.50	101.2	180.1	84.20	116.1	96.70	117.9	132.2	108.4	116.8	93.90	117.1	46.00	38.20
Zr	153.3	456.7	13.70	76.40	50.00	84.70	86.80	130.1	321.5	586.7	317.6	546.9	513.9	647.6	436.1	372.7	283.1	336.2	681.1	146.4	117.8
Elemental Ratio																					
V/V+Ni	0.89	0.92	0.93	0.94	0.90	0.83	0.92	0.84	0.87	0.86	0.99	0.92	0.91	0.92	0.97	0.95	0.93	0.96	0.90	0.60	0.24
V/Cr	2.45	2.69	0.46	3.76	3.24	2.71	4.35	2.40	1.95	2.42	9.48	4.30	3.79	4.41	5.97	7.00	4.37	5.33	4.07	0.41	0.22
Ca/Ca+Fe	0.91	0.99	0.66	0.95	0.97	0.93	0.93	0.86	0.69	0.23	0.34	0.10	0.51	0.34	0.15	0.09	0.55	0.28	0.25	0.81	0.69
Fe/Ca+Mg	0.06	0.36	0.01	0.05	0.03	0.07	0.07	0.14	0.42	2.10	1.26	2.77	0.71	1.28	2.77	6.56	0.78	2.19	2.02	0.20	0.26
Ti/Al	0.13	0.05	0.16	0.12	0.11	0.14	0.14	0.16	0.16	0.16	0.15	0.16	0.16	0.17	0.17	0.12	0.16	0.12	0.18	0.25	0.23
Na/K	2.98	1.17	42.60	3.23	3.77	1.16	0.86	1.99	1.41	1.51	0.41	0.77	0.98	0.92	0.88	3.69	2.89	4.21	1.30	3.80	5.91
K/Fe+Mg	0.02	0.11	0.00	0.04	0.10	0.11	0.21	0.04	0.06	0.05	0.13	0.15	0.14	0.16	0.10	0.03	0.03	0.02	0.12	0.04	0.01
Sr/Ba	1.91	0.89	7.11	2.67	2.65	1.27	1.13	1.90	2.59	0.86	0.06	0.74	0.65	0.40	1.44	0.45	1.06	0.54	0.39	0.98	1.62

Table 5.3 Major oxides, minor and trace element concentration in various lithofacies of Ninama Basin. (NS/NL/1-3 GBL facies, NS/NL/4-9 CL and ML facies, NS/SF/10-17 SH facies, NS/SF/18 SM facies, NS/SF/19-21 LGW facies)

5.3.2 CHOTILA BASIN

A total of 66 samples were analyzed, which comprises, 27 samples of Bamanbor Formation (19 of CS, 4 of SS, 4 of FSS facies), 30 samples of Chotila Chert (17 of LC and MC, 14 of MS facies) and 9 samples of Rangpar Formation (9 of CS facies) (Table 5.4, 5.5, 5.6, 5.7, 5.8). Average concentration of selected major oxides, minor and trace elements of the different lithofacies of Chotila Basin are mentioned in the subsequent paragraph which are used for to calculate the elemental ratios which are further used to interpret the paleoenvironmental parameters of deposition of the various lithofacies of the Chotila Basin. Remaining data of the minor and trace elements of the each lithofacies has also been tabulated (Table 5.3) that gives full length of information of the each lithofacies.

In the Bamanbor Formation, the CS facies, consists of SiO_2 ranging from 42% to 74% (avg. 51.88wt.%), CaO ranging from 1% to 7% (avg. 3.206 wt.%), Fe_2O_3 ranging from 7% to 16% (avg. 12.18 wt.%), Al_2O_3 ranging from 9% to 17% (avg. 14.38 wt.%), MgO ranging from 1% to 7.5% (avg. 3.01wt.%), Na_2O ranging from 0.5% to 2.9% (1.38 wt.%), Ti ranging from 0.5% to 1.8% (avg. 1.33 wt.%), Mn ranging from 0.01% to 0.18% (avg. 0.06 wt.%), Sr ranging from 91 ppm to 215 ppm (avg. 140.53 ppm), Zr ranging from 118.9 ppm to 505 ppm (avg. 304.65 ppm), Rb ranging from 7.3 ppm to 206.6 ppm (avg. 67.226 ppm), and value of other elements are shown in Table 5.4; the SS facies consists of SiO_2 ranging from 46% to 54% (avg. 48.83 wt.%), CaO ranging from 1.4% to 2.6% (avg. 2.08 wt.%), Fe_2O_3 ranging from 6% to 15% (avg. 12.79 wt.%), Al_2O_3 ranging from 13% to 16% (avg. 15.33 wt.%), MgO ranging from 2% to 4% (avg. 3.314 wt.%), Na_2O ranging from 1% to 2% (1.78 wt.%), Ti ranging from 0.5% to 1.9% (avg. 1.47 wt.%), Mn ranging from 0.05% to 0.15% (avg. 0.104 wt.%), Sr ranging from 146 ppm to 226 ppm (avg. 188.8 ppm), Zr ranging from 368 ppm to 1150 ppm (avg. 608.7 ppm) and Rb ranging from 10 ppm to 64.8 ppm (avg. 50.275 ppm), and value of other elements are shown in Table 5.5 and the FSS facies consists of SiO_2 ranging from 37% to 49% (avg. 45.52 wt.%), CaO ranging from 2% to 15% (avg. 5.43 wt.%), Fe_2O_3 ranging from 12% to 15% (avg. 13.715 wt.%), Al_2O_3 ranging from 13% to 16% (avg. 14.82 wt.%), MgO ranging from 0.1% to 6.9% (avg. 1.42 wt.%), Na_2O ranging from 1.7% to 2.1% (1.95 wt.%), Ti ranging from 1.4% to 1.8% (avg. 1.6 wt.%), Mn ranging from 0.08% to 0.74% (avg. 0.26 wt.%), Sr ranging from 230 ppm to 363 ppm (avg. 294.6 ppm), Zr ranging from 353 ppm to 385 ppm (avg. 369.22 ppm), Rb ranging from 52 ppm to 56 ppm (avg. 54.6 ppm), and value of other elements are shown in Table 5.5.

In the Chotila Chert, the LC and MC facies, consists of SiO_2 ranging from 64% to 96% (avg. 88.69 wt.%), CaO ranging from 0.1% to 1.7% (avg. 0.73 wt.%), Fe_2O_3 ranging from 1% to 11% (avg. 3.93 wt.%), Al_2O_3 ranging from 0.07% to 11.84% (avg. 4.39 wt.%), MgO ranging from 7% to 10% (avg. 6.67 wt.%), Na_2O ranging from 0.05% to 1% (0.48 wt.%), Ti ranging from 0.08% to 0.8% (avg. 0.34 wt.%), Mn ranging from 0.002% to 0.079% (avg. 0.0183 wt.%), Sr ranging from 18.6 ppm to 502.1 ppm (avg. 144.97 ppm), Zr ranging from 23 ppm to 338.3 ppm (avg. 101.21 ppm), Rb ranging from 2 ppm to 128.3 ppm (avg. 31.51 ppm) and value of other elements are shown in Table 5.6, and the MS facies consists of SiO_2 46% to 69% (avg. 57.04 wt.%), CaO ranging from 0.6% to 8.7% (avg. 2.58 wt.%), Fe_2O_3 ranging from 5% to 16% (avg. 9.93 wt.%), Al_2O_3 ranging from 8% to 20% (avg. 13.87 wt.%), MgO ranging from 1.5% to 5.1% (avg. 3 wt.%), Na_2O ranging from 0.6% to 3.88% (1.34 wt.%), Ti ranging from 0.53% to 2% (avg. 1 wt.%), Mn ranging from 0.01% to 0.22% (avg. 0.08 wt.%), Sr ranging from 65 ppm to 484 ppm (avg. 163.13 ppm), Zr ranging from 87 ppm to 566 ppm (avg. 290.02 ppm), Rb ranging from 3 ppm to 176 ppm (avg. 76.84 ppm), and value of other elements are shown in Table 5.7.

In the Rangpar Formation, the CS facies consists of SiO_2 39% to 74% (avg. 55.63 wt.%), CaO ranging from 0.6% to 9.3% (avg. 3.66 wt.%), Fe_2O_3 ranging from 8% to 17% (avg. 12.27 wt.%), Al_2O_3 ranging from 8.1% to 13.6% (avg. 11.02 wt.%), MgO ranging from 1.2% to 3% (avg. 2.3 wt.%), Na_2O ranging from 0.9% to 2% (1.69 wt.%), Ti ranging from 0.85% to 2.11% (avg. 1.42 wt.%), Mn ranging from 0.01% to 0.24% (avg. 0.07 wt.%), Sr ranging from 96 ppm to 385 ppm (avg. 175.55 ppm), Zr ranging from 163 ppm to 309 ppm (avg. 227.25 ppm), Rb ranging from 19.1 ppm to 60.7 ppm (avg. 33.41 ppm), and value of other elements are shown in Table 5.8. These elements are associated with minerals like quartz, clay minerals pyrite, hematite and calcite.

5.3.2.1 Paleosalinity

The elemental ratio of Ca/Ca+Fe of Bamanbor Formation for CS facies is 0.20, for SS facies is 0.14, for FSS facies is 0.23; the ratio for MS facies of Chotila Chert, is 0.20 and for LC and MC facies are 0.16 and for CS facies of Rangpar Formation is 0.21. The ratio of Ca/(Ca+Fe) for all the lithofacies suggests their deposition in freshwater conditions (Fig. 5.5a) (He *et al.* 2017; Khan *et al.* 2023).

The elemental ratios of Sr/Ba, of Bamanbor Formation for CS facies is 0.78, for SS facies is 0.59, for FSS facies is 0.50; the ratio for MS facies of Chotila Chert, is 0.54 and for LC and MC facies are 1.5 and for CS facies of Rangpar Formation is 2.6. The Sr/Ba ratio suggests the deposition of CS and SS facies of Bamanbor formation and MS facies of Chotila Chert in brackish water; while deposition of FSS facies in freshwater, and the deposition of LC/MC facies in saline water (Fig. 5.5b) (Wei and Algeo 2020; Gu *et al.* 2022).

Due to stratigraphic temporal evolution of these elemental ratios a wider range of the paleosalinity is considered for the basin, where the deposition of CS facies of Rangpar Formation in a freshwater to brackish water environment, is followed by deposition of MS facies and MC and LC facies in a fresh to saline and fresh to brackish water, respectively; while the deposition of FSS facies suggests a freshwater condition in the basin, followed by fresh to brackish water conditions during the deposition of SS and CS facies of Bamanbor Formation (Fig. 5.5a, b).

5.3.2.2 Paleoredox conditions

The elemental ratio of V/V+Ni of Bamanbor Formation for CS facies is 0.88 (anoxic), for SS facies is 0.82 (anoxic), for FSS facies is 0.79 (suboxic); the ratio for MS facies of Chotila Chert, is 0.87 (anoxic) and for LC and MC facies are 0.93 (anoxic) and for CS facies of Rangpar Formation is 0.89 (anoxic) (Fig. 5.5c). The ratio of V/Cr, of Bamanbor Formation for CS facies is 6.21 (anoxic), for SS facies is 5.01 (anoxic), for FSS facies is 1.45 (oxic); the ratio for MS of Chotila Chert, is 5.52 (anoxic) and for LC and MC facies are 4.59 (anoxic) and for CS facies of Rangpar Formation is 5.4 (anoxic) (Fig. 5.5d).

The elemental ratios for both the paleoredox indicators, V/V+Ni and V/Cr show nearly similar results. Initially, the deposition of CS facies of Rangpar Formation and deposition of MC and LC and MS facies of Chotila Chert, shows anoxic conditions, gradually changing to oxic during the deposition of FSS facies of Bamanbor formation and again followed by anoxic conditions during the deposition of SS and CS facies of Bamanbor Formation (Fig. 5.5c, d).

5.3.2.3 Paleodepth

The elemental ratio of Fe/(Ca+Mg) of Bamanbor Formation for CS facies is 2.52, for SS facies is 3.08, for FSS facies is 1.60; the ratio for MS facies of Chotila Chert, is 2.35 and for LC and MC facies are 3.30 and for CS facies of Rangpar Formation is 3.00 (Fig. 5.5e). The overall values of Fe/Ca+Mg suggest rather, a deep lacustrine system, which is also reflected in

the lithofacies. The shallowing of the basin during the deposition of FSS facies of Bamanbor Formation is also corroborated with the deposition of coarse-grained sediments followed by an increase in the paleodepth of the basin during the deposition of SS and CS facies of Bamanbor Formation (Fig. 5.5e).

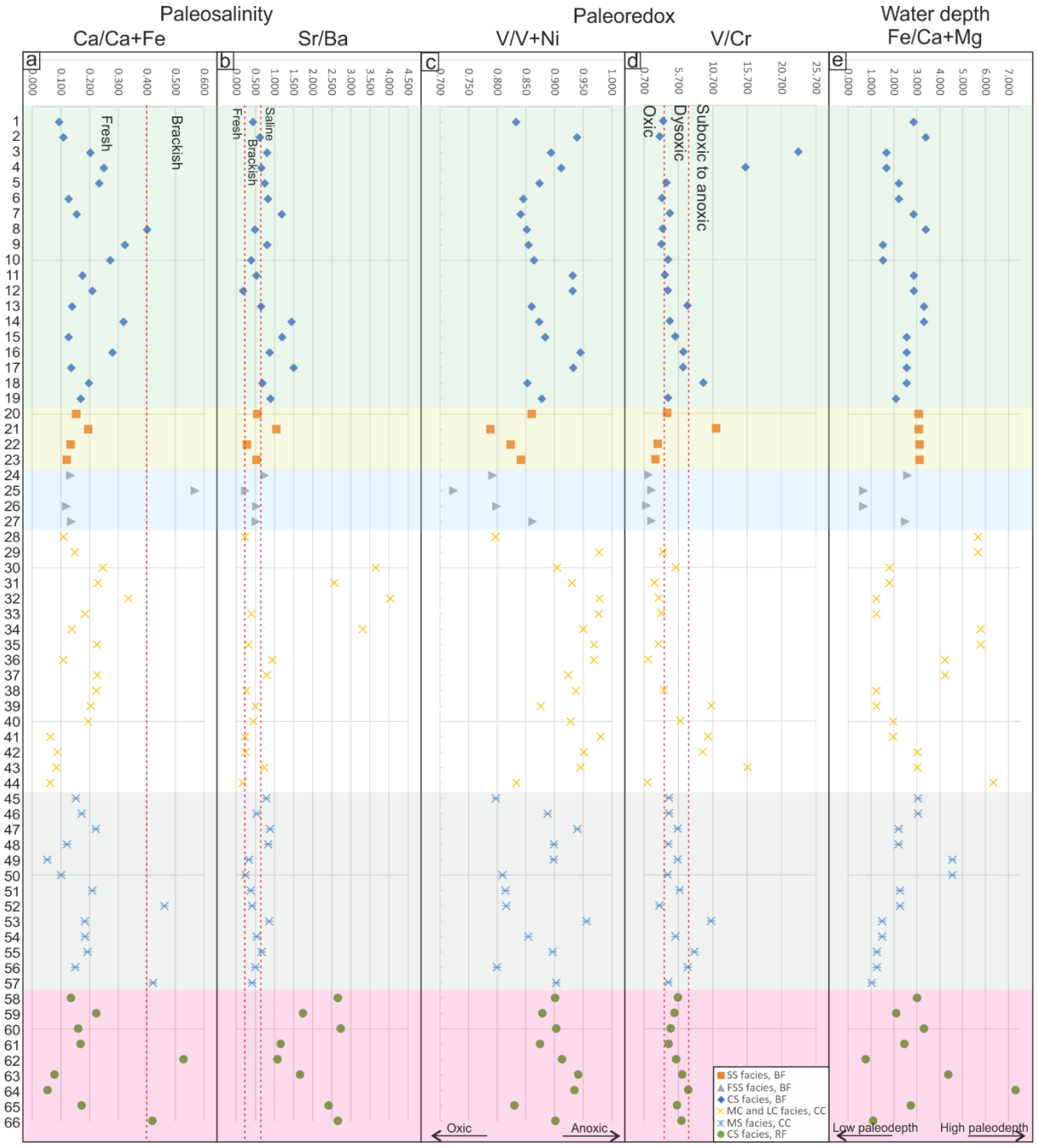

Fig. 5.5, Plot of the geochemical proxies for paleosalinity, a. Ca/(Ca+Fe), a. Sr/Ba; paleoredox c. V/V+Ni, d. V/Cr; paleodepth and, e. Fe/(Ca+Mg), of the Chotila Basin.

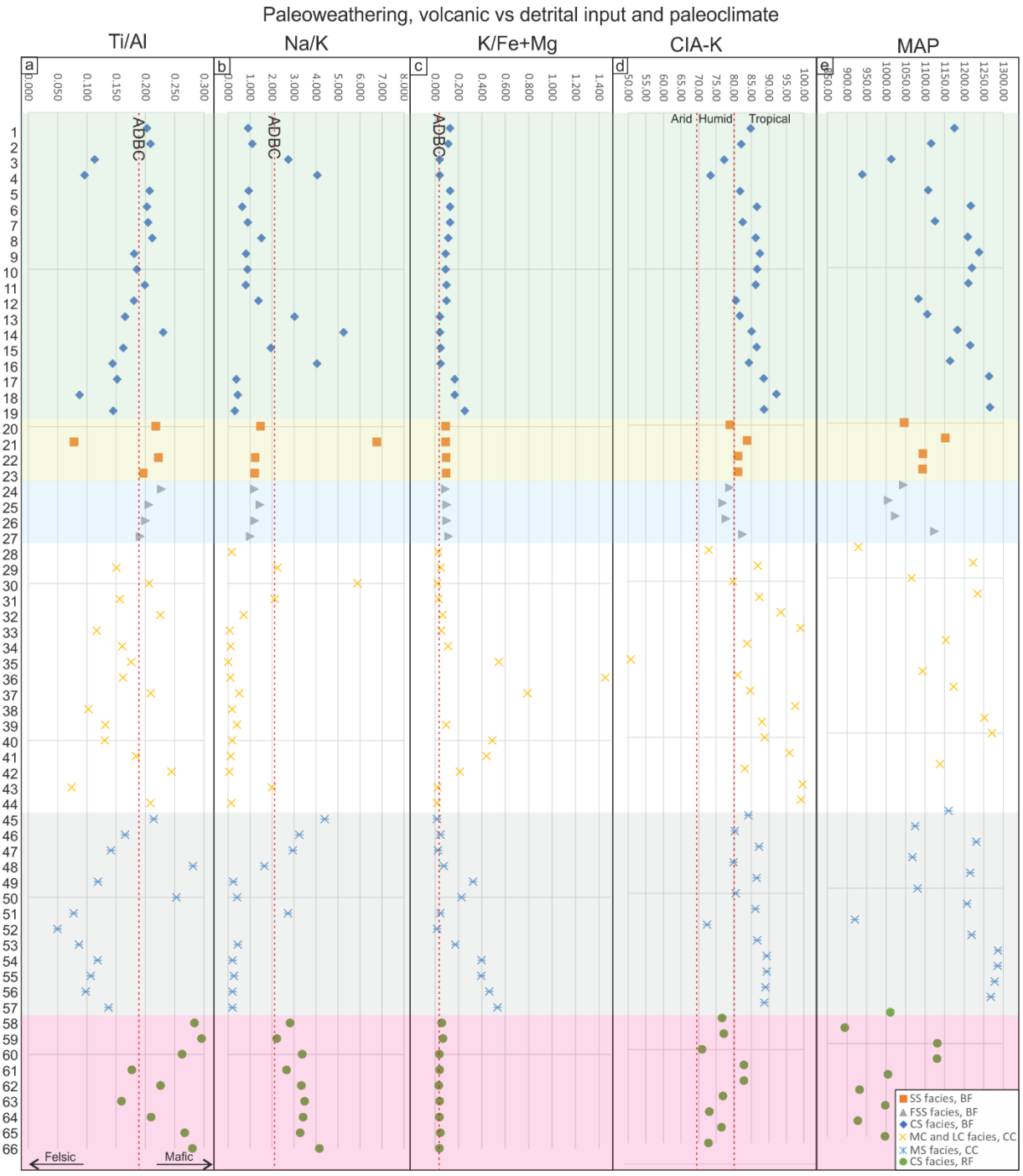

Fig. 5.6 Plot of the geochemical proxies for paleoweathering, volcanic vs detrital input and paleoclimate, a. Ti/Al, b. Na/K, c. K/Fe+Mg, d. Al/Ti, e. CIA-K, and f. MAP, of the Chotila Basin.

5.3.2.4 Paleoweathering and paleoclimatic conditions

The average values of Ti/Al of Bamanbor Formation for CS facies is 0.17, for SS facies is 0.17, for FSS facies is 0.20; the ratio for MS facies of Chotila Chert, is 0.13 and for LC and MC facies are 0.27 and for CS facies of Rangpar Formation is 0.21. The high Ti/Al values are indicative of mafic composition of the host rocks and relatively high rate of detrital input in the basin. The ratios of CS, SS, FSS facies are closer to the Ti/Al values of Average Deccan Basalt Composition (ADBC) 0.19, as given by Crocket and Paul (2004)) (Fig. 5.6a).

The CIA-K average value of Bamanbor Formation for CS facies is 85.95, for SS facies is 81.23, for FSS facies is 79.01; the value for MS facies of Chotila Chert, is 84.64 and for LC and MC facies are 86.58 and for CS facies of Rangpar Formation is 76.59. The CIA-K average values for various lithofacies suggest a humid-tropical climate) (Fig. 5.6d).

CIA-K values were also used to calculate the Mean Annual Precipitation (MAP) to understand the intensity of weathering linked to the quantity of precipitation. The MAP values average 1209.39 mm, 1095.55 mm and 1049.14 mm for CS, SS and FSS facies respectively, of Bamanbor Formation, 1176.31mm and 1245.77 mm for MS and MC and LC facies respectively, of Chotila Chert and 1001.90 mm for CS facies of Rangpar Formation. The higher values over 1000 mm are suggestive of relatively high precipitation) (Fig. 5.6e).

Sample No.	BRC/BF/19	BRC/BF/20	BRC/BF/2	BRC/BF/4	BRC/BF/6	BRC/BF/7	BRC/BF/8	RGIDC/BF/3	RGIDC/BF/4	RGIDC/BF/5	RGIDC/BF/6	RGIDC/BF/8	RGIDC/BF/10	RRI/BF/1	RRI/BF/2	RRI/BF/4	CHS/BF/1	CHS/BF/3	CHS/BF/4
MAJOR OXIDE																			
SiO_2	48.73	51.04	48.18	55.69	46.01	52.10	47.96	42.65	44.48	45.84	47.01	44.34	48.45	45.28	63.08	74.34	61.88	58.64	60.08
Al_2O_3	16.86	16.53	13.65	16.21	16.38	15.27	16.46	14.11	14.08	14.39	15.28	15.99	16.13	13.95	11.61	8.90	11.38	12.88	13.25
Fe_2O_3	16.81	13.16	14.33	13.62	14.13	13.63	13.59	11.89	12.45	11.24	14.54	14.53	13.19	10.86	8.40	8.04	10.20	7.69	9.25
MnO	0.14	0.06	0.21	0.18	0.23	0.07	0.12	0.15	0.06	0.07	0.05	0.06	0.04	0.06	0.04	0.02	0.02	0.05	0.02
MgO	2.48	2.64	5.71	7.53	2.41	3.24	2.62	2.94	2.58	2.58	2.29	1.82	2.16	3.40	2.39	1.64	2.77	3.14	2.95
CaO	1.70	1.57	3.56	4.44	4.22	1.94	2.44	7.78	5.82	4.10	3.02	3.76	2.08	4.96	1.20	3.06	1.57	1.84	1.85
Na_2O	1.51	1.79	2.01	2.93	1.82	1.18	1.73	1.12	1.01	1.10	1.21	1.92	1.80	1.22	0.91	0.83	0.74	0.55	0.85
K_2O	1.48	1.46	0.65	0.64	1.73	1.66	1.72	0.66	1.11	1.11	1.35	1.24	0.53	0.21	0.42	0.18	1.78	1.11	2.52
TiO_2	3.01	3.05	1.36	1.38	2.99	2.73	2.97	2.64	2.25	2.36	2.68	2.55	2.36	2.84	1.66	1.13	1.53	0.99	1.70
P_2O_5	0.21	0.29	0.13	0.14	0.40	0.19	0.22	0.17	0.14	0.12	0.18	0.17	0.09	0.89	0.15	0.18	0.11	0.13	0.19
Total	92.92	91.60	89.79	102.76	90.32	92.01	89.83	84.11	83.98	82.91	87.62	86.38	86.84	83.67	89.84	98.32	91.96	87.03	92.66
CIA-K	84.82	82.17	77.28	73.45	81.82	86.58	82.61	86.27	87.44	86.70	86.32	80.68	81.72	85.13	86.51	84.33	88.51	92.13	88.59
MAP	1175.05	1115.41	1013.00	939.26	1107.63	1216.67	1125.13	1209.11	1237.42	1219.38	1210.30	1082.99	1105.50	1182.4	1215	1163.9	1263.59	1357.17	1265.79
MINOR AND TRACE ELEMENTS																			
Al	89210	87510	72270	85790	86680	80820	87140	74660	74520	76170	80890	84640	85360	73830	61440	47120	60230	68150	70130
Ba	319.1	197.7	199.3	277.2	259.5	167.2	180.0	215.7	142.7	338.0	248.3	896.9	259.4	115.3	102.8	139.6	60.7	156.2	102.5
Ca	12140	11210	25450	31760	30140	13880	17470	55600	41600	29330	21590	26900	14850	35450	8542	21870	11220	13180	13180
Co	36.0	10.3	32.1	31.8	20.0	20.7	34.5	26.0	15.4	18.6	< 7.8	< 6.2	28.6	51.2	31.2	7.7	< 2.3	29.8	37.3
Cr	90.3	90.2	12.8	21.0	65.0	92.6	61.5	95.6	84.0	73.6	85.3	76.7	67.5	88.8	56.1	45.7	42.1	8.2	50.2
Cs	9.5	10.4	7.4	10.8	11.7	13.9	< 1.0	12.7	12.4	9.5	9.5	12.8	10.7	11.7	14.5	< 1.0	11.1	14.8	20.4
Cu	92.8	79.9	113.4	169.2	88.1	129.0	82.8	80.7	85.7	93.2	88.0	98.6	157.9	206.0	81.9	80.5	71.2	36.6	78.8
Fe	117500	92030	100200	95290	98800	95340	95030	83140	87110	78620	101700	101600	92250	75940	58720	56230	71350	53770	64680
Ga	29.3	26.4	19.9	19.5	25.7	24.3	28.6	22.7	24.1	25.1	22.7	23.3	26.7	21.1	20.9	15.6	20.8	27.1	23.3
Hf	7.7	< 3.9	5.4	< 3.6	< 2.0	5.0	< 3.9	3.5	4.6	< 3.4	< 4.1	< 2.0	8.2	< 3.1	3.1	4.1	< 3.1	11.4	< 2.9
K	12300	12100	5435	5349	14360	13750	14260	5491	9178	9201	11220	10320	4432	1721	3459	1514	14760	9192	20920

Mg	14940	15940	34410	45390	14550	19510	15780	17720	15550	15520	13810	10970	13030	20520	14390	9890	16670	18940	17790
Nb	59.9	61.6	9.7	9.0	58.3	56.4	88.4	46.2	44.1	49.8	59.1	42.6	31.5	20.4	31.4	18.3	29.3	71.8	31.1
Ni	62.7	17.2	35.2	31.5	36.8	55.7	51.6	56.0	45.6	48.5	23.2	23.3	76.6	57.2	38.7	17.0	19.4	13.2	29.1
Pb	13.4	10.1	6.0	5.2	8.7	10.0	14.1	12.7	9.4	9.5	7.2	6.0	14.5	11.1	8.7	9.8	7.7	38.3	8.5
Rb	71.3	72.9	17.2	11.6	86.3	86.2	88.0	35.5	76.8	77.0	85.8	65.3	28.8	7.3	28.8	11.4	162.5	58.0	206.6
Sc	26.0	30.6	47.3	53.5	34.3	31.0	29.9	33.7	33.0	30.9	28.7	27.4	31.0	36.6	22.5	17.9	25.2	17.9	26.5
Sr	139.0	122.8	161.2	181.5	193.2	138.5	215.3	105.8	114.8	132.9	131.0	162.1	168.8	167.5	123.7	122.1	91.4	106.8	91.7
Th	11.1	10.0	4.8	3.6	7.6	9.5	15.7	9.4	10.6	9.3	8.6	8.4	12.0	6.9	8.3	4.7	6.7	28.0	6.6
Ti	18050	18260	8174	8249	17940	16370	17820	15810	13480	14130	16090	15280	14120	17000	9968	6791	9142	5952	10180
U	2.8	< 0.4	1.1	1.2	2.1	3.5	1.8	< 1.1	1.4	0.6	< 1.3	2.1	2.4	1.9	1.0	2.1	< 0.9	3.3	2.6
V	312.6	265.9	295.8	324.1	254.0	305.0	272.7	320.9	268.0	308.4	315.1	316.9	471.1	392.7	294.2	292.0	268.6	76.4	209.0
Y	30.8	41.6	20.7	11.1	54.9	33.5	60.0	35.9	31.8	33.0	41.5	41.8	34.3	74.0	33.7	5.4	35.0	83.5	43.4
Zn	139.9	132.3	85.9	97.1	140.3	134.7	140.3	131.3	72.9	59.7	125.0	93.3	128.2	112.5	91.0	34.8	80.1	138.3	96.6
Zr	375.3	390.2	118.9	136.2	375.8	347.3	505.5	323.9	322.9	349.0	378.8	310.0	275.3	205.6	248.9	157.7	219.4	500.6	247.1
ELEMENTAL RATIOS																			
V/V+Ni	0.833	0.939	0.894	0.911	0.873	0.846	0.841	0.851	0.855	0.864	0.931	0.932	0.860	0.873	0.884	0.945	0.933	0.853	0.878
V/Cr	3.462	2.948	23.109	15.433	3.908	3.294	4.434	3.357	3.190	4.190	3.694	4.132	6.979	4.422	5.244	6.389	6.380	9.317	4.163
Ca/Ca+Fe	0.094	0.109	0.203	0.250	0.234	0.127	0.155	0.401	0.323	0.272	0.175	0.209	0.139	0.318	0.127	0.280	0.136	0.197	0.169
Fe/Ca+Mg	2.858	3.390	1.674	1.674	2.211	2.211	2.858	3.390	1.524	1.524	2.873	2.873	3.309	3.309	2.561	2.561	2.558	2.558	2.088
Ti/Al	0.202	0.209	0.113	0.096	0.207	0.203	0.204	0.212	0.181	0.186	0.199	0.181	0.165	0.230	0.162	0.144	0.152	0.087	0.145
Na/K	0.911	1.099	2.738	4.062	0.940	0.639	0.901	1.517	0.817	0.890	0.801	1.377	3.019	5.253	1.943	4.049	0.371	0.444	0.303
K/Fe+Mg	0.129	0.112	0.040	0.040	0.127	0.127	0.129	0.112	0.089	0.089	0.097	0.097	0.042	0.042	0.047	0.047	0.168	0.168	0.254
Sr/Ba	0.436	0.621	0.809	0.655	0.745	0.828	1.196	0.490	0.804	0.393	0.528	0.181	0.651	1.453	1.203	0.875	1.506	0.684	0.895

Table 5.4 Major oxides, minor and trace element concentration in Clay Shale facies, Bamanbor Formation.

Sample No.	BRC/BF/9	BRC/BF/11	BRC/BF/12	BRC/BF/23	BRC/BF/14	BRC/BF/22	BRC/BF/16	BRC/BF/17
MAJOR OXIDE								
SiO_2	46.1	54.59	47.19	47.47	46.88	37.65	47.77	49.78
Al_2O_3	15.8	13.67	16.52	15.33	15.08	13.04	14.83	16.35
Fe_2O_3	15.35	6.128	15.49	14.23	14.72	12.12	15.16	12.86
MnO	0.2064	0.07061	0.1408	0.1241	0.1088	0.9654	0.1672	0.1086
MgO	2.623	3.775	3.037	3.14	3.139	2.591	3.981	3.647
CaO	2.683	1.451	2.322	1.87	2.206	15.58	1.991	1.98
Na_2O	2.115	1.325	1.918	1.783	2.025	1.959	2.114	1.73
K_2O	1.299	0.1756	1.398	1.334	1.519	1.211	1.564	1.547
TiO_2	3.032	0.9371	3.236	2.651	3.024	2.37	2.617	2.752
P_2O_5	0.1872	< 0.00069	0.2782	0.2683	0.314	0.7496	0.2904	0.3109
Total	89.3956	82.12231	91.53	88.2004	89.0158	88.236	90.4846	91.0655
CIA-K	78.88168	83.76225	81.15543	81.12828	78.82906	76.89586	77.81509	82.53407
MAP	1045.376	1150.877	1093.266	1092.681	1044.293	1005.27	1023.64	1123.365
MINOR AND TRACE ELEMENTS								
Al	83630	72340	87460	81140	79840	69020	78480	86520
Ba	381.4	216.8	535.5	340	493.1	1158	438.8	620.1
Ca	19180	10370	16600	13360	15770	111300	14230	14150
Co	33.9	23.6	20.5	31.1	23.8	21.7	32.4	18
Cr	85.7	3.3	131.5	111.7	251.9	140.9	317.3	179.7
Cs	9.5	16.3	9.1	10.1	8.4	10.7	10.8	11
Cu	87.7	8.6	87.9	70.8	56.5	47.1	44.3	51.9
Fe	107300	42860	108300	99510	102900	84790	106000	89980
Ga	26	31.6	27.9	28.8	22.9	19.1	24.5	22
Hf	5.7	15.7	< 2.0	5	< 4.2	4.4	< 4.0	< 3.9

K	1078	1458	1161	11070	1261	10050	1298	12840
Mg	15820	22760	18310	18930	18930	15620	24000	21990
Nb	59.3	212.7	60	89.9	54.5	59.8	49.9	54.9
Ni	56.1	9.9	74.4	48.3	86.4	94	82.7	50.1
Pb	13.9	21.3	9.1	18.6	7.7	11	9.5	9.7
Rb	64.8	10	63.4	62.9	56.6	53	52.6	56.2
Sc	28.4	15.4	31.2	27.2	29.7	21	32.5	27.5
Sr	206.9	226.2	146.4	175.7	363.2	267.4	230.3	317.5
Th	94000	299000	89000	179000	91000	87000	75000	88000
Ti	1.818	0.5617	1.939	1.589	1.813	1.42	1.569	1.65
U	2.6	5.5	1	3.7	3.4	1.1	1.7	3.1
V	343	36.7	344.7	255.2	328	245.6	327.8	312.2
Y	34.1	85.1	39.6	59.7	36.6	89.8	41.7	48.7
Zn	111.4	146.3	154.4	119.5	141.8	116.2	129.9	112.8
Zr	368.2	1150	391.9	524.7	353.7	374.5	385.7	363
ELEMENTAL RATIOS								
V/V+Ni	0.859	0.788	0.822	0.841	0.792	0.723	0.799	0.862
V/Cr	4.002	11.121	2.621	2.285	1.302	1.743	1.033	1.737
Ca/Ca+Fe	0.152	0.195	0.133	0.118	0.133	0.568	0.118	0.136
Fe/Ca+Mg	3.066	3.066	3.102	3.102	2.582	0.668	0.668	2.490
Ti/Al	0.217	0.078	0.222	0.196	0.227	0.206	0.200	0.191
Na/K	1.455	6.742	1.226	1.194	1.191	1.446	1.208	1.000
K/Fe+Mg	0.088	0.088	0.092	0.092	0.089	0.100	0.100	0.115
Sr/Ba	0.542	1.043	0.273	0.517	0.737	0.231	0.525	0.512

Table 5.5 Major oxides, minor and trace element concentration in Silty shale and fossiliferous shaly sandstone facies, Bamanbor Formation.

Sample No.	RGIDC/ CC/2	RGIDC/ CC/15	RGIDC/ CC/16	RGIDC/ CC/17	RGIDC/ CC/18	CHSE/ CC/7	CHSE/ CC/8	CHSE/ CC/9	CHSE/C C/10	CHSE/C C/12	BNR/C C/1	CHSW/ CC/2	CHSW/ CC/4	CHSW/ CC/7	CHSW /CC/9	RRI/CC /7	RRI/C C/8
MAJOR OXIDE																	
SiO_2	95.81	91.57	86.51	95.91	89.40	92.59	86.95	95.17	82.49	84.48	95.46	64.86	91.73	93.58	74.44	90.40	96.48
Al_2O_3	0.08	5.19	5.71	2.41	2.76	2.72	4.63	1.55	9.23	4.05	1.13	11.84	3.56	2.47	7.16	6.97	3.28
Fe_2O_3	3.11	2.83	5.15	2.58	1.70	3.33	2.71	1.70	1.60	6.96	4.97	7.26	4.06	3.88	11.41	2.59	1.06
MnO	0.09	0.00	0.03	0.01	0.00	0.00	0.01	0.00	0.01	0.04	0.04	0.03	0.01	0.02	0.10	0.00	0.00
MgO	0.20	1.05	1.38	0.54	0.60	0.87	0.36	0.36	0.98	3.59	0.53	2.25	0.59	1.06	6.99	1.40	< 0.016
CaO	0.37	0.48	1.64	0.75	0.84	0.95	0.32	0.49	0.45	1.75	0.32	1.72	0.27	0.37	1.03	0.57	0.17
Na_2O	0.01	0.39	0.72	0.18	0.10	0.01	0.45	0.75	1.07	0.37	0.01	0.81	0.23	0.05	0.72	0.01	0.01
K_2O	0.08	0.16	0.11	0.07	0.12	1.87	3.70	1.33	5.37	0.81	0.08	3.79	1.69	0.85	0.32	0.17	0.10
TiO_2	0.14	0.69	1.04	0.33	0.55	0.42	0.66	0.29	0.84	0.47	0.21	1.36	0.58	0.53	0.47	0.72	0.46
P_2O_5	0.05	0.14	0.26	0.02	0.12	0.03	0.06	0.02	0.03	0.10	0.05	0.11	0.03	0.03	0.09	< 0.002	0.17
Total	99.93	102.50	102.55	102.79	96.20	102.81	99.85	101.66	102.06	102.60	102.79	94.02	102.75	102.84	102.74	102.83	101.73
CIA-K	72.89	86.85	79.82	87.30	93.45	98.98	83.87	50.74	81.16	84.72	97.58	88.02	88.79	95.83	83.18	99.60	99.15
MAP	929.07	1222.94	1064.96	1233.96	1392.87	1553.23	1153.41	600.45	1093.42	1172.69	1510.8	1251.49	1270.68	1459.71	1137.6	1572.2	1558.5
MINOR AND TRACE ELEMENTS																	
Al	398.6	27470	30240	12730	14620	36890	17350	14400	24500	8201	48850	21410	62660	18860	13090	37890	5964
Ba	84.00	63.60	77.20	69.40	82.50	145.50	151.60	124.10	103.10	93.70	269.80	146.40	249.70	196.30	158.50	117.10	148.50
Ca	2638	3440	11700	5342	5995	4085	1180	6796	2300	3488	3229	12470	12310	1916	2619	7375	2297
Co	11.40	< 3.0	22.40	< 5.9	< 0.2	< 0.9	< 4.3	< 0.7	< 2.8	< 5.5	< 3.9	19.60	28.60	7.30	8.50	12.10	16.90
Cr	1533.00	78.60	54.10	64.70	62.50	64.30	161.60	121.90	251.00	451.30	45.00	39.70	43.60	32.90	31.10	29.50	283.50
Cs	12.10	16.80	14.60	10.40	12.90	16.80	20.90	12.80	13.70	< 1.0	12.80	19.90	< 1.0	21.70	12.70	13.00	10.50
Cu	35.60	41.00	80.90	40.50	42.10	29.90	28.10	52.30	82.50	36.70	104.20	148.70	80.90	56.00	46.30	53.70	59.00
Fe	21740	19780	36000	18020	11900	18090	7382	23290	18960	11890	11210	48690	50760	28370	27140	79820	34760
Ga	4.60	11.80	10.10	6.80	7.80	12.70	8.90	7.00	7.50	3.80	8.30	11.60	24.90	9.50	8.00	15.50	6.50
Hf	< 2.0	< 2.3	4.00	< 2.0	< 2.0	< 1.5	< 2.0	< 2.0	< 2.1	< 2.0	< 2.0	< 2.6	7.10	< 2.3	< 2.2	< 3.0	< 2.0

K	629	1301	911	611	1020	1375	829	15540	30710	11070	44560	6682	31430	14040	7063	2697	670
Mg	1201	6310	8340	3282	3628	8440	98	5250	2174	2167	5900	21650	13550	3570	6380	42170	3184
Nb	2.70	12.60	15.70	7.10	9.70	17.30	10.50	7.20	9.30	4.90	24.60	8.80	47.40	10.70	7.50	8.70	3.90
Ni	36.90	6.20	30.40	10.70	4.00	4.80	5.00	10.90	10.30	13.20	10.80	58.90	20.20	6.60	14.80	27.00	66.20
Pb	3.30	7.80	8.20	5.10	5.50	2.10	6.10	5.10	5.70	3.30	4.70	6.50	18.90	5.50	4.80	6.50	5.00
Rb	2.00	6.00	6.60	5.50	4.30	8.80	5.10	42.90	62.10	27.70	109.20	17.70	128.30	59.60	32.90	10.90	6.20
Sc		8.80	11.50	9.30				8.50	10.80		10.40	9.30	23.20			11.00	
Sr	18.60	428.50	282.10	178.30	332.90	58.20	502.10	40.50	97.30	75.10	71.30	73.80	111.60	44.10	38.30	86.10	25.70
Th	2.10	5.40	6.10	3.80	4.20	5.50	4.30	2.00	3.70	2.10	7.40	2.70	18.00	4.20	3.20	2.10	1.40
Ti	817	4141	6237	1988	3290	4309	2781	2531	3963	1714	5017	2817	8171	3467	3200	2810	1245
U	2.80	3.10	3.80	2.20	3.80	0.60	5.00	1.20	3.50	1.60	2.80	0.70	1.90	2.40	2.30	< 0.8	3.30
V	145.00	269.90	287.20	142.90	175.70	202.50	94.40	337.60	321.70	160.00	160.90	413.90	259.80	328.40	287.00	464.10	330.60
Y	3.60	4.40	35.30	4.10	4.30	8.20	7.70	4.20	5.80	2.90	16.10	12.30	73.20	7.60	7.00	18.30	8.10
Zn	11.20	18.40	53.10	17.80	24.40	24.10	8.70	22.30	27.30	17.90	56.30	86.40	96.80	32.40	28.30	41.40	73.90
Zr	23.20	106.10	117.00	62.50	78.80	178.30	71.80	58.70	70.50	48.70	226.00	75.30	338.30	89.70	54.80	80.20	40.70
ELEMENTAL RATIOS																	
V/V+Ni	0.80	0.98	0.90	0.93	0.98	0.98	0.95	0.97	0.97	0.92	0.94	0.88	0.93	0.98	0.95	0.95	0.83
V/Cr	0.09	3.43	5.31	2.21	2.81	3.15	0.58	2.77	1.28	0.35	3.58	10.43	5.96	9.98	9.23	15.73	1.17
Ca/Ca+Fe	0.11	0.15	0.25	0.23	0.34	0.18	0.14	0.23	0.11	0.23	0.22	0.20	0.20	0.06	0.09	0.08	0.06
Fe/Ca+Mg	5.66	5.66	1.80	1.80	1.24	1.24	5.78	5.78	4.24	4.24	1.23	1.23	1.96	1.96	3.02	3.02	6.34
Ti/Al	2.05	0.15	0.21	0.16	0.23	0.12	0.16	0.18	0.16	0.21	0.10	0.13	0.13	0.18	0.24	0.07	0.21
Na/K	0.16	2.24	5.88	2.12	0.70	0.07	0.12	0.01	0.11	0.50	0.18	0.41	0.19	0.12	0.06	1.99	0.15
K/Fe+Mg	0.03	0.05	0.02	0.03	0.07	0.05	0.11	0.54	1.45	0.79	2.60	0.09	0.49	0.44	0.21	0.02	0.02
Sr/Ba	0.22	6. 74	3.65	2.57	4.04	0.40	3.31	0.33	0.94	0.80	0.26	0.50	0.45	0.22	0.24	0.74	0.17

Table 5.6 Major oxides, minor and trace element concentration in massive chert and laminated chert facies, Chotila Chert.

Sample No.	RGIDC/CC/11	RGIDC/CC/13	RGIDC/CC/14	RGIDC/CC/20	CHSE/CC/5	CHSE/CC/11	BNR/CC/2	BNR/CC/3	CHSW/CC/1	CHSW/CC/3	CHSW/CC/5	CHSW/CC/6	CHSW/CC/8
MAJOR OXIDE													
SiO_2	48.75	56.96	69.81	51.39	67.40	46.38	51.76	52.92	54.53	62.05	59.33	61.21	59.11
Al_2O_3	13.04	12.21	8.68	13.45	13.37	14.77	19.52	20.37	12.65	13.60	13.99	12.72	11.97
Fe_2O_3	14.57	8.83	7.72	12.32	12.39	16.46	11.91	10.38	7.83	6.61	5.36	7.36	7.39
MnO	0.14	0.22	0.02	0.28	0.06	0.08	0.29	0.13	0.04	0.07	0.04	0.04	0.05
MgO	2.52	2.42	1.53	2.41	2.38	4.32	2.41	5.19	2.17	3.03	3.46	3.36	3.85
CaO	2.56	1.80	2.14	1.66	0.66	1.81	3.10	8.71	5.57	1.15	1.25	1.63	1.63
Na_2O	1.23	1.50	0.64	1.69	1.04	1.78	1.57	3.88	0.97	0.81	0.83	0.78	0.76
K_2O	0.25	0.41	0.19	0.92	3.95	3.84	0.51	0.22	4.37	3.59	2.78	3.45	1.56
TiO_2	2.47	1.78	1.08	3.34	1.40	3.30	1.33	0.89	1.53	1.18	1.32	1.33	0.92
P_2O_5	0.29	0.21	0.18	0.27	0.11	0.19	0.07	0.13	0.11	0.21	0.18	0.18	0.17
Total	85.82	86.35	92.00	87.73	102.75	92.92	92.47	102.82	89.76	92.29	88.54	92.06	87.40
CIA-K	84.17	80.28	87.17	79.94	86.50	80.55	86.18	72.41	86.67	89.41	89.38	89.09	88.68
MAP	1160.21	1074.49	1230.82	1067.31	1214.74	1080.34	1207.04	920.31	1218.67	1286.44	1285.60	1278.19	1267.95
MINOR AND TRACE ELEMENTS													
Al	69010	64640	45970	71200	70740	78180	103300	107800	63370	67340	74070	71990	66950
Ba	215.2	319	86.3	578.7	195.3	584.3	422.9	353.9	190.9	287.3	266.3	261.8	203
Ca	18290	12860	15320	11870	4722	12920	22140	62230	11610	11640	8930	8186	39800
Co	49.1	73	< 3.1	20.8	37.7	43	21.1	15.7	27.3	18.7	21.6	26.1	11.2
Cr	86.3	65.7	55.1	97.6	54.5	173.5	55.4	66.6	9.9	35.7	13.6	13.4	52.3
Cs	9.6	9.9	16.1	10.2	< 1.0	14.1	14	3.7	12.3	13.9	12.6	14.4	11.7
Cu	177.8	93.9	70.3	131.1	105.3	288.5	125.6	79.2	41.8	88.7	50.3	52.4	79.4
Fe	101900	61740	53980	86130	86640	115100	83320	72560	51700	51500	37510	46230	54760
Ga	22.4	22.4	15.7	22.6	20.2	27.4	23.4	14.3	24.3	22.4	28.2	27.2	20.7
Hf	< 3.4	< 2.0	< 2.0	< 2.0	12.7	< 2.0	< 2.0	< 2.0	11	12	13.7	9.3	< 3.0

K	2072	3432	1613	7612	32750	31840	4269	1858	12920	28620	23040	29820	36270
Mg	15180	14620	9220	14500	14320	26020	14540	31280	23200	20270	20880	18240	13060
Nb	24.2	36.2	21.3	40.2	24.9	21.6	9.6	5	69	54.9	81.1	70.3	32
Ni	94.7	35.9	19.7	46.5	34.3	168.1	74	44.1	4.8	32.1	12.5	23.7	23.7
Pb	13.7	7.8	7.8	11.2	12.5	11.8	9.2	5.9	28.5	17.9	24.1	22.5	7.2
Rb	13.2	29	12.2	55.9	169.1	90.2	18.5	3.5	71.5	111.4	117.7	130.5	176.3
Sc	25.40	23.80	20.20	34.00	26.90	37.90	57.50	58.80	18.60	26.80	21.60	12.70	
Sr	169.3	169.7	76.4	484.4	65	140.7	158.5	146.9	164.7	153.1	176.9	131.1	84
Th	6.9	8.7	5.9	11.4	5.8	3.7	4.7	4.5	25.7	22.2	31.3	27	6.9
Ti	14790	10690	6478	20030	8400	19770	7998	5339	5498	7977	7905	7079	9168
U	3.2	< 0.4	1.3	4.7	3.5	1.9	< 0.4	< 0.4	3.6	2.4	6.3	3.8	0.4
V	372.6	283.7	306.3	412.5	303.2	712.9	324.3	195.1	103.2	188	108.6	94.5	220.3
Y	41.7	41.9	11.3	35.6	25.9	62.3	21.1	14.3	82.8	80.4	88.4	88.9	28.2
Zn	133.6	103	44.5	95.8	88.8	212.4	83.3	53.1	143.8	129.9	142.6	153	70.8
Zr	209	278.4	161.6	275.5	237.6	213	119.1	87.4	481.1	397.8	566.1	491.7	252
ELEMENTAL RATIOS													
V/V+Ni	0.80	0.89	0.94	0.90	0.90	0.81	0.81	0.82	0.96	0.85	0.90	0.80	0.90
V/Cr	4.32	4.32	5.56	4.23	5.56	4.11	5.85	2.93	10.42	5.27	7.99	7.05	4.21
Ca/Ca+Fe	0.15	0.17	0.22	0.12	0.05	0.10	0.21	0.46	0.18	0.18	0.19	0.15	0.42
Fe/Ca+Mg	3.04	3.04	2.20	2.20	4.55	4.55	2.27	2.27	1.49	1.49	1.26	1.26	1.04
Ti/Al	0.21	0.17	0.14	0.28	0.12	0.25	0.08	0.05	0.09	0.12	0.11	0.10	0.14
Na/K	4.39	3.24	2.94	1.64	0.24	0.42	2.72	15.48	0.44	0.20	0.27	0.20	0.20
K/Fe+Mg	0.02	0.04	0.03	0.08	0.32	0.23	0.04	0.02	0.17	0.40	0.39	0.46	0.53
Sr/Ba	0.79	0.53	0.89	0.84	0.33	0.24	0.37	0.42	0.86	0.53	0.66	0.50	0.41

Table 5.7 Major oxides, minor and trace element concentration in mudstone facies, Chotila Chert.

Sample No.	RGIDC/RF/21	RGIDC/RF/23	RGIDC/RF/25	RGIDC/RF/28	GRS/RF/1	GRS/RF/3	GRS/RF/5	GRS/RF//7	GRS/RF/9
MAJOR OXIDE									
SiO_2	48.30	45.89	51.21	63.92	58.91	74.82	69.88	48.01	39.77
Al_2O_3	13.60	13.50	10.64	10.74	9.09	10.19	8.18	12.55	10.72
Fe_2O_3	12.27	12.42	17.90	10.02	8.57	10.93	12.81	13.15	12.44
MnO	0.12	0.09	0.22	0.02	0.02	0.04	0.02	0.03	0.32
MgO	2.54	2.79	2.36	2.42	2.11	1.86	1.21	2.46	3.01
CaO	1.86	3.49	3.32	1.97	9.34	0.89	0.70	2.66	8.74
Na_2O	2.07	2.00	2.18	1.11	0.94	1.54	1.51	1.93	2.01
K_2O	0.66	0.81	0.58	0.38	0.25	0.40	0.40	0.53	0.43
TiO_2	3.40	3.52	2.46	1.67	1.81	1.43	1.51	2.96	2.65
P_2O_5	0.21	0.26	0.11	0.65	0.32	0.25	0.32	0.12	0.20
Total	85.03	84.77	90.99	92.90	91.36	102.34	96.53	84.39	80.28
CIA-K	76.65	77.15	70.91	82.84	82.83	76.82	73.04	76.49	72.77
MAP	1010.35	893.53	1130.26	1129.84	1003.86	931.68	997.21	926.74	996.27
MINOR AND TRACE ELEMENTS									
Al	71990	71470	56340	56840	48090	53930	43270	66420	56730
Ba	67.40	55.50	88.70	111.00	121.80	96.40	48.30	45.80	56.00
Ca	1.33	2.49	2.37	1.41	6.68	0.63	0.50	1.90	6.24
Co	20.10	23.10	15.50	38.30	< 5.4	10.10	22.30	34.90	26.90
Cr	74.20	77.20	80.70	62.90	64.60	57.00	65.70	66.90	62.90
Cs	7.80	10.40	9.40	21.10	14.50	16.40	11.40	11.10	10.50
Cu	176.20	159.30	119.20	115.10	98.90	90.60	104.10	189.40	145.30
Fe	85840	86890	125200	70110	59900	76470	89600	92000	86970
Ga	24.60	25.40	21.10	17.60	16.80	17.60	14.70	21.60	20.90
Hf	5.40	4.20	< 4.4	2.80	< 2.0	< 2.0	11.80	6.20	< 3.1

K	5472	6751	4829	3114	2106	3285	3296	4393	3599
Mg	15300	16810	14250	14620	12710	11190	7310	14840	18130
Nb	46.40	43.70	31.70	25.50	25.10	28.00	23.50	33.50	28.80
Ni	45.80	54.10	39.40	38.20	32.90	22.20	32.60	75.00	42.00
Pb	6.90	9.10	12.10	7.30	10.00	10.20	10.20	9.90	7.70
Rb	48.40	60.70	28.30	19.10	20.80	23.00	25.80	38.60	36.00
Sc	26.50	37.30	25.00	25.90		11.00	14.00	25.10	31.00
Sr	178.90	96.30	242.30	127.90	130.50	159.90	385.40	110.30	148.50
Th	8.20	7.20	5.70	4.60	5.60	4.70	6.80	5.00	6.70
Ti	20400	21110	14770	10020	10830	8554	9043	17710	15860
U	1.20	0.60	< 0.4	1.00	1.80	1.90	4.50	< 0.4	< 0.9
V	413.60	389.20	363.70	265.80	343.00	351.90	463.90	363.60	381.70
Y	32.90	38.40	17.50	62.10	32.00	22.00	11.20	44.20	29.30
Zn	100.80	95.70	52.80	79.10	94.80	63.20	53.90	152.10	82.10
Zr	309.50	284.60	217.90	217.90	174.10	213.60	163.20	252.00	212.50
ELEMENTAL RATIOS									
V/V+Ni	0.90	0.88	0.90	0.87	0.91	0.94	0.93	0.83	0.90
V/Cr	5.57	5.04	4.51	4.23	5.31	6.17	7.06	5.43	6.07
Ca/Ca+Fe	0.13	0.22	0.16	0.17	0.53	0.08	0.05	0.17	0.42
Fe/Ca+Mg	3.00	2.08	3.30	2.44	0.75	4.36	7.30	2.72	1.08
Ti/Al	0.28	0.30	0.26	0.18	0.23	0.16	0.21	0.27	0.28
Na/K	2.81	2.20	3.35	2.65	3.32	3.47	3.40	3.26	4.13
K/Fe+Mg	0.05	0.07	0.03	0.04	0.03	0.04	0.03	0.04	0.03
Sr/Ba	2.65	1.74	2.73	1.15	1.07	1.66	7.98	2.41	2.65

Table 5.8 Major oxides, minor and trace element concentration in Clay Shale facies, Rangpar Formation.